

**NIST GCR 97-719**

---

---

**SEISMIC RISK ANALYSIS OF LIQUID FUEL  
SYSTEMS: A Conceptual and Procedural  
Framework for Guidelines Development**

---

---

Building and Fire Research Laboratory  
Gaithersburg, Maryland 20899

**NIST**

United States Department of Commerce  
Technology Administration  
National Institute of Standards and Technology

NIST GCR 97-719

---

---

SEISMIC RISK ANALYSIS OF LIQUID FUEL  
SYSTEMS: A Conceptual and Procedural  
Framework for Guidelines Development

---

---

M. Shinozuka  
University of Southern California  
and  
Ronald Eguchi  
EQE International, Inc.

A report to:  
U.S. Department of Commerce  
Technology Administration  
National Institute of Standards and Technology  
Building and Fire Research Laboratory  
Gaithersburg, MD 20899

June, 1997



U.S. Department of Commerce  
William M. Daley, *Secretary*  
Technology Administration  
Gary R. Bachula, *Acting Under Secretary for Technology*  
National Institute of Standards and Technology  
Robert E. Hebner, *Acting Director*

## PREFACE

The Congressional emergency appropriation resulting from the January 17, 1994 Northridge earthquake provided the Building and Fire Research Laboratory (BFRL) at the National Institute of Standards and Technology (NIST) an opportunity to increase its activities in earthquake engineering under the National Earthquake Hazard Reduction Program (NEHRP). In addition to the post-Northridge earthquake reconnaissance, BFRL concentrated its efforts primarily in the study of post-earthquake fire and lifelines, and moment resisting steel frames.

BFRL sponsored a post-earthquake fire and lifelines workshop in Long Beach, California in January 1995 to assess technology development and research needs that will be used in developing recommendations to reduce the effects of post-earthquake fires. The workshop participants developed a list of priority project areas where further research, technology development, or information collection and dissemination would serve as a vital step in reducing the losses from post-earthquake fires. NIST funded a number of studies identified by the participants which are listed in NIST Special Publication 889.

BFRL, working with practicing engineers, carried out surveys and assessment of the damaged buildings and partially funded a SAC (Structural Engineers Association of California, Applied Technology Council, California Universities for Research in Earthquake engineering) workshop on seismic performance of steel frame buildings in September 1994. The objectives of the workshop were threefold: 1) to coordinate related interests; 2) focus on the problems observed in the performance of steel buildings; and 3) develop a research plan to solve the problems. NIST funded the research and engineering communities to carry out several of the proposed studies.

This report represents a part of these studies related to post-earthquake fire and lifelines sponsored by NIST as part of the Congressional emergency appropriation.

## ABSTRACT

Recent earthquakes, notably the 1989 Loma Prieta, 1994 Northridge and 1995 Hyogoken Nanbu (Kobe) earthquakes, caused widespread damage to the urban infrastructure facilities including lifeline networks. The unacceptable seismic performance of many lifelines during these earthquakes creates an urgent need to develop comprehensive seismic design and retrofit guidelines. Most current design and construction standards for lifelines do not include seismic provisions and those that do, focus on the seismic performance of components, such as pipelines, pumping stations, and storage tanks. There are neither seismic design guidelines nor codes that apply to lifelines as a whole, particularly from the systems point of view. The guidelines developed for a particular component may permit design or retrofit in accordance with a specific level of seismic risk that is not consistent with the importance of that component when analyzed from a systems point of view. In fact, a joint National Institute of Standards and Technology (NIST) and Federal Emergency Management Agency (FEMA) effort to develop and adopt seismic design guidelines and standards for lifelines concluded that "standards for lifeline design and construction must give special attention to the performance of each lifeline as a system and to the interdependence of the various lifeline systems".

This study develops a conceptual and procedural framework for design and retrofit guidelines for liquid fuel systems. To focus the study and to ensure a useful result in a limited time-frame, however, this study concentrates on seismic performance of oil transmission systems. Within this context, the study still emphasizes the systems aspect of the lifeline and takes into consideration explicitly the lifeline system performance and economic losses resulting from service disruptions. Ground work will be laid for the development of design and retrofit guidelines for oil transmission systems by following the framework thus estimated. Such guidelines will enhance the integrity of oil transmission systems in a seismic event and will minimize the direct and indirect economic losses resulting from loss of service.

# TABLE OF CONTENTS

	PREFACE.....	iii
	ABSTRACT.....	v
	TABLE OF CONTENTS.....	vii
	LIST OF TABLES.....	ix
	LIST OF FIGURES.....	xi
	ACKNOWLEDGEMENT.....	xiii
Section 1	<b>INTRODUCTION.....</b>	<b>1</b>
	BACKGROUND.....	1
	OUTLINE OF STUDY.....	2
Section 2	<b>PERFORMANCE OF GAS AND LIQUID FUEL PIPELINE SYSTEMS.....</b>	<b>5</b>
	HISTORIC PERFORMANCE OF GAS AND LIQUID FUEL PIPELINE SYSTEMS DURING EARTHQUAKES.....	5
Section 3	<b>COMPONENT FRAGILITY MODELS.....</b>	<b>13</b>
	FUNCTIONAL HIERARCHY.....	13
	COMPONENT FRAGILITY.....	13
Section 4	<b>SYSTEMS FRAGILITY MODELS.....</b>	<b>17</b>
	SYSTEMS ANALYSIS.....	17
	SOCIO-ECONOMIC LOSS AND SYSTEM FRAGILITY.....	19
	BENEFIT-COST ANALYSIS.....	21
	ACCEPTABLE LOSS.....	21
Section 5	<b>SEISMIC DESIGN AND RETROFIT GUIDELINES.....</b>	<b>23</b>
	UNCERTAINTY ANALYSIS.....	23
	RELIABILITY ALOCATION.....	23
	FRAMEWORK FOR PROTOTYPE DESIGN AND RETROFIT GUIDELINES.....	24
Section 6	<b>AN EXAMPLE OF ECONOMIC LOSS.....</b>	<b>27</b>
	HAZARD DATA.....	27
	PIPELINE MODEL.....	28
	APPLICATION OF LIBRARY MODELS.....	29
	RESULTS.....	30
Section 7	<b>CONCLUSIONS AND RECOMMENDATIONS.....</b>	<b>35</b>
Section 8	<b>REFERENCES.....</b>	<b>37</b>

## LIST OF TABLES

Table 1.	Earthquakes Included In The Performance Summary In Reverse Chronological Order.....	39
Table 2.	Earthquakes Included In The Performance Summary In Order of Decreasing Magnitude.....	40
Table 3.	Damage Categories of Selected Earthquakes.....	41
Table 4.	Damage Probability Matrix Based on Expert Opinion for Low-rise Reinforced Concrete Shear-Wall Buildings (with Moment-Resisting Frame).....	42
Table 5.	Pipeline Exposure in a Magnitude 8.6 Earthquake in the NMSZ (Thousands of Feet) .....	43
Table 6.	Remediation of Cost Schedule for all Models.....	44

## LIST OF FIGURES

Figure 1.	Schematic fault tree- like depiction of an oil transmission system .....	45
Figure 2.	A family of component fragility curves .....	46
Figure 3.	NEHRP Seismic Map Areas (BSSC, 1988).....	47
Figure 4.	Damage percent by intensity for petroleum fuels distribution storage tanks .....	48
Figure 5.	Residual capacity for petroleum fuels distribution storage tanks (NEHRP California 7) .....	49
Figure 6.	Residual capacity for petroleum fuels distribution storage tanks (NEHRP Map Area: California 3-6, Non-California 7, and Puget Sound 5).....	50
Figure 7.	Residual capacity for petroleum fuels distribution storage tanks (All other areas).....	51
Figure 8.	Residual capacity of crude oil delivery from Texas and Louisiana to Chicago following New Madrid event (M=8.0) .....	52
Figure 9a.	Simplified Restoration curves .....	53
Figure 9b.	Actual restoration curves for different water delivery systems .....	53
Figure 10.	Seismic hazard function, $H(m)$ , and seismic hazard density, $h(m) = -dH(m)/dm$ , and expected conditional economic loss, $L(m)$ .....	54
Figure 11.	Optimal level of design guideline upgrading .....	55
Figure 12.	Optimal strategy and level of retrofit .....	56
Figure 13.	Flow chart for development of design guidelines .....	57
Figure 14.	Flow chart for execution of retrofit procedures.....	58
Figure 15.	Component fragility curves.....	59
Figure 16.	Modified Mercalli Intensity For a Magnitude 8.6 Event Anywhere Along the New Madrid Seismic Zone. (Digitized from Algermissen and Hopper, 1984) .....	60
Figure 17.	Areas of Moderate to High Liquefaction Potential in the New Madrid Seismic Zone During a Major Earthquake. (Digitized from Obermeier, 1985) .....	61

## ACKNOWLEDGMENTS

The authors wish to acknowledge the support provided by the National Institute of Standards and Technology (NIST) to complete this study. They also wish to express their gratitude for the interest expressed, advice given and exhaustive review of the draft report carried out by the NIST staff, including Richard N. Wright, H.S. Lew, Riley M. Chung and Bijan Mohraz. In particular, Bijan Mohraz was helpful as the technical monitor for this study throughout the grant period.

## SECTION 1 INTRODUCTION

### BACKGROUND

Recent earthquakes, notably the 1989 Loma Prieta, 1994 Northridge and 1995 Hyogoken Nanbu (Kobe) earthquakes, caused widespread damage to the urban infrastructure including lifeline networks. The unacceptable seismic performance of many lifelines during these earthquakes creates an urgent need to develop comprehensive seismic design and retrofit guidelines. Most current design and construction standards for lifelines do not include seismic provisions and those that do, focus on the seismic performance of components, such as pipelines, pumping stations, and storage tanks. There are neither seismic design guidelines nor codes that apply to lifelines as a whole, particularly from the systems point of view. The guidelines developed for a particular component may permit design or retrofitting in accordance with a specific level of seismic risk that is not consistent with the importance of that component when analyzed from a systems point of view. In fact, a joint National Institute of Standards and Technology (NIST) and Federal Emergency Management Agency (FEMA) effort to develop and adopt seismic design guidelines and standards for lifelines (Dijkers et al., 1996 & FEMA, 1995) concluded that "standards for lifeline design and construction must give special attention to the performance of each lifeline as a system and to the interdependence of the various lifeline systems".

This FEMA-NIST plan for developing and adopting seismic design and construction guidelines and standards for lifelines was prepared in response to Public Law 101-614, the National Earthquake Hazards Reduction Program (NEHRP) Reauthorization Act of 1990. The act required the FEMA, in consultation with the NIST, to develop "a plan... for developing and adopting... design and construction standards for lifelines" and "recommendations of ways Federal regulatory authority could be used to expedite the implementation of such standards".

The Plan is primarily based on the technical input of experts from the private and public sectors who participated in a workshop held September 25-27, 1991, in Denver, Colorado. Those experts determined that design guidelines and standards are needed to reduce the vulnerability of lifelines to earthquakes and that adequate knowledge bases exist or can be developed to produce them. Under this plan, the development of the guidelines and their adoption as standards will be carried out in two stages. In the first phase, a Lifeline Seismic Safety

Executive Board is established and charged with the responsibility of developing the pre-standards, and in the second phase, consensus standards are developed from the pre-standards for voluntary adoption by owner-agencies.

The FEMA-NIST Plan was submitted to the U.S. Congress in September 1995 and estimates that it will take eight to ten years to complete standards for all five lifelines (electric power, gas and liquid fuels, telecommunications, transportation, and water supply and wastewater systems). As noted above, the successful completion of this plan depends on the availability of "adequate knowledge" and/or the generation of this knowledge. The subject project will address one of the largest gaps in the knowledge base, namely the evaluation of lifeline systems performance and the establishment of rational performance criteria for these systems.

This study reviews the past seismic performance of liquid fuel systems and develops a conceptual and procedural framework for the design and retrofit guidelines for liquid fuel systems. To focus the study and to ensure a useful result in a limited time-frame, however, this study concentrates on seismic performance of oil transmission systems. Within this context, the study still emphasizes the systems aspect of the lifeline and takes into consideration explicitly the lifeline system performance and economic losses resulting from service disruptions. Ground work will be laid for the development of design and retrofit guidelines for oil transmission systems by following the framework thus estimated. Such guidelines will enhance the integrity of oil transmission systems in a seismic event and will minimize the direct and indirect economic losses resulting from loss of service. Furthermore, the study will develop meaningful performance criteria such as minimum acceptable levels of service at defined time periods following earthquakes of different sizes.

## OUTLINE OF STUDY

This report consists of seven sections dealing primarily with earthquake performance of oil transmission systems. Section 2 which follows the introductory remarks in Section 1 describes the past performance of oil transmission pipeline systems under various earthquakes. In Section 3, earthquake fragility functions for components of oil transmission pipeline facilitates are introduced and those developed in ATC-13 (Applied Technology Council, 1988) and ATC-25 (Applied Technology Council, 1991) loss estimation studies are reviewed. Section 4 shows that these fragility functions will be modified as appropriate and utilized in the development of

system fragility models for the transmission systems. Section 4 also indicates how system fragility analysis can be performed on the basis of the fault tree network constructed uniquely from the oil transmission system configuration. The system fragilities are then defined in terms of expected conditional economic loss. In principle, then, performance criteria are defined by thresholds of expected annual economic loss. Reviewing and summarizing the results obtained in Sections 2-4, significant seismic design and retrofit considerations that must be examined will be delineated in Section 5. Section 6 demonstrates an example of economic loss arising from environmental contamination caused by leakage of oil out of seismically induced pipe breaks in a crude oil transmission systems passing through the New Madrid Seismic Zone. Finally, Section 7 will provide conclusions and recommendations for future study to further enhance the art and science of seismic design of lifeline systems in general and oil transmission systems in particular.

Throughout this study, probabilistic approach will be used in order to introduce the uncertainty and randomness involved in the analytical models, the parameters therein, and the earthquake phenomena into the analysis in a rational fashion. In this study, an oil transmission system is considered as a collection of components which perform their respectively unique functions required by the system as a whole to perform its ultimate function. The probabilistic approach calls for (1) development of component fragility curves, (2) development of a fault tree depiction of the system in order to identify functional hierarchy of and interrelationship among the components, (3) systems analysis under a scenario earthquake with various values of magnitude using Monte Carlo simulation techniques, and (4) development of restoration curves and estimation of attendant direct and indirect losses in terms of expected conditional and annual economic losses. The guidelines for seismic design and retrofit of lifeline systems can be established so as to bring the estimated loss close to the acceptable loss as much as possible.

**BLANK PAGE**

## **SECTION 2**

### **PERFORMANCE OF GAS AND LIQUID FUEL PIPELINE SYSTEMS**

In order to fully understand the range of effects that are possible during an earthquake, it is useful to investigate and document earthquake damage in actual events. The purpose of the following review is to document earthquake damage to gas and liquid fuel facilities during U.S. and worldwide earthquakes. In addition, short summaries of failures occurring during normal operations are discussed.

#### **HISTORIC PERFORMANCE OF GAS AND LIQUID FUEL PIPELINE SYSTEMS DURING EARTHQUAKES**

The performance of underground pipelines in earthquakes has ranged from extremely poor to good. The most significant damage has resulted in areas of large permanent ground failure, including fault rupture and liquefaction. This section provides a summary of the historic performance of liquid fuel pipelines and facilities, including both oil and natural gas, in selected earthquakes. Natural gas facilities have been included because the pipelines behave in essentially the same manner as oil pipelines.

Data on earthquake-induced damage has been collected following most major earthquakes in modern times. For earthquakes occurring before 1960, however, this information is not as readily available. Information on early events has been derived from historic accounts some of which provide an indication of system performance.

Forty-six significant earthquakes from around the world were selected including 41 "modern" earthquakes (i.e., those well-studied earthquakes occurring after 1960), and 5 earlier, but noteworthy events. Five of the earthquakes are of Richter Magnitude 8.0 or greater, twenty between M7.0 and 7.9, fourteen are between M6.0 and 6.9, and seven measured less than M6.0. Table 1 lists these events chronologically, and Table 2 presents them in order of decreasing magnitude.

Facilities included in the damage summary are: natural gas pipelines (transmission and distribution), oil transmission pipelines, and facilities using and storing liquid fuels (refineries, pumping plants, tank farms) and associated equipment (storage tanks and piping, etc.). The

earthquakes have been categorized by the amount of damage that occurred. Three categories have been used: significant damage, minor to moderate damage, and no damage reported. Table 3 presents the damage categorizations for the selected events.

Significant damage was noted in five events. These earthquakes were of varied magnitude and location. An oil transmission pipeline suffered serious damage in the 1987 Ecuador Earthquake (M = 6.9). Oil refineries were heavily damaged in two Japanese events; the 1978 Miyagi-Ken-Oki (M = 7.4) and the 1964 Niigata (M = 7.5) earthquakes. In 1978, oil spill damage at a refinery and a collapsed propane tank led to serious power outages. In Niigata, fires at refineries caused significant damage. In the 1971 San Fernando Earthquake (M = 6.6), gas service to 17,000 customers was disrupted by damage to several gas transmission pipelines. Tank farms and storage facilities were among the hardest hit structures in the 1964 Alaska Earthquake (M = 8.4).

In the 1989 Loma Prieta earthquake (M=7.1), the natural gas distribution system suffered \$19 million in damages. More recently, two earthquakes had a significant effect on gas and liquid fuel systems. The Northridge earthquake (M=6.7), which occurred on January 17, 1994, caused significant damage to gas transmission (35 repairs) and distribution (154) pipelines. Exactly one year later, the Kobe earthquake (M=6.9) damaged both medium-pressure and low-pressure pipelines, with over 26,000 repairs to the low-pressure system.

Moderate to minor damage was reported in 17 other earthquakes, and the remaining 18 events had no damage reported. Damage reports for events which caused minor damage to liquid fuel facilities often provided little useful information. Although the fire damage caused by the 1906 San Francisco Earthquake is infamous, it has been classified as "moderate" because little reliable information exists on direct damage to liquid fuel facilities. Table 3 presents the damage categories for each of the 40 selected earthquakes.

The following is a brief summary of the damage sustained in each earthquake categorized as producing significant damage to liquid fuel pipelines.

#### **1995 Kobe (M=6.9)**

The Kobe earthquake (or more formally known as the Hyogoken Nanbu earthquake) caused considerable damage and destruction to all lifeline systems. Particularly hard hit were

transportation systems (including highways, railways and port facilities), and water and natural gas distribution networks. Gas supply to around 900,000 households was shutoff after the earthquake due to extensive damage to medium-pressure gas pipelines, and low-pressure pipeline systems including service connections and meter sets (Shinozuka et al., 1995). Approximately 100 repairs were made to medium pressure pipelines, while over 5000 repairs were made to main and branch systems. In addition, over 10,000 service lines were damaged and about 11,000 service connections to buildings were severed or damaged. Perhaps most compelling was the time required to fully repair the gas distribution system. It took roughly three months to restore service to those structures that could receive service. The total expense associated with this restoration effort is estimated at 190 billion yen, or approximately \$2.3 billion (Shinozuka et al., 1995). It is noted that this total covers network repair, replacement, administration, and related activities.

#### **1994 Northridge (M=6.7)**

Following the Northridge earthquake, approximately 151,000 gas outages (out of 4.7 million customers) were reported by the Southern California Gas Company (SoCal Gas, 1994). The large majority of these outages were due to customer-initiated shut off. According to SoCal Gas records, roughly 120,000 services were restored within three weeks; the remaining customers were inaccessible because of earthquake damage to structures or for other reasons. In total, SoCal Gas responded to over 400,000 customer requests after the earthquake. According to SoCal Gas reports, the Northridge earthquake caused the following pipe failures or leaks: Steel transmission pipelines (35 repairs), distribution pipelines (154 repairs), plastic pipelines (27), leaks on meter sets (6,461) and leaks on customer facilities (15,021). According to company statistics compiled for 1993, there are 3,803 miles of steel transmission pipelines, and 26,809 miles and 14,935 miles of steel and plastic distribution mains, respectively. Most of the problems in transmission pipe appear to have been related to the performance of pre-1932 oxy-acetylene-welded steel pipe.

#### **1989 Loma Prieta (M=7.1)**

While the regional natural gas transmission system was virtually undamaged, just 2 leaks were reported and repaired without customer interruption, the distribution systems in several areas were severely impacted. Over 1,000 pipeline leaks were reported system-wide, and three low-pressure systems were so heavily damaged that replacement was required. Replacement

consisted primarily of insertion of plastic pipe into existing mains and services. The distribution system in the Marina District of San Francisco was replaced within one month, at a cost of \$17 million. 5,100 customers were affected. Reconstruction of the Watsonville low pressure system was complete within three weeks, affecting 166 customers. 140 customers were impacted in Los Gatos, where main restoration was accomplished within 10 days, and service restoration was complete within a month. Total gas system damages have been estimated at \$32 million (Phillips and Virostek, 1990).

Most of the region's refineries and tank farms are located along the Bay in Alameda or Contra Costa Counties. Numerous tanks at soft-soil sites were damaged, predominantly those tanks that were full or nearly full. Typical damage models included; elephant's foot buckling, sometimes associated with loss of contents; damage to associated piping; and uplift of unanchored tank walls. It was reported that all leaks were contained within containment dikes, and that no fires resulted (EERI, 1990).

#### **1987 Ecuador (M = 6.9)**

Earthquake-induced mudslides caused serious damage to the Trans-Ecuadorian pipeline, the largest single pipeline loss in history (Crespo, 1987). This pipeline, built in 1972, is a 26-inch diameter X-60 grade steel pipe that carries oil 260 miles from the Ecuadorian oil fields east of the Andes to the Pacific Ocean port of Esmeraldas. Approximately 250,000 barrels per day flow through this pipeline. Along the Coca River, 6.5 miles of the T-E pipeline were completely destroyed. Localized mud flows damaged 10 miles of pipeline and severed it in at least 8 places. Five additional miles were deformed with significant distortion and displacement of above-ground pipeline supports. A pipeline bridge across the Aquarico River, 30 miles west of the oil field was destroyed by flooding and dislodged 2 miles of the pipeline from support structures. Lost revenue and the cost of reconstruction totaled \$1-1.5 billion dollars (Crespo, 1987). The Poliducto Pipeline, an 8" natural gas pipeline following approximately the same route as the Trans-Ecuadorian pipeline, suffered damages in the same locations. In addition, a landslide toppled a storage tank at the Salado Pump Station, spilling 4,500 barrels of crude oil.

#### **1978 Miyagi-Ken-Oki/Sendai, Japan (M = 7.4)**

At the Sendai Refinery, belonging to the Tohoku Oil Company, three out of 87 large tanks

holding refined fuel failed, spilling 68,100 kiloliters of oil. Because the surrounding containment dikes could only accommodate 35,000 kl, the oil overtopped the dike, inundating much of the refinery area and spilling over into the port. The oil drained rapidly due to failure at the base of the tanks, creating a vacuum which caused the three tanks to implode. Three other tanks were damaged, but did not fail. Serious fires were averted because, at the time of the earthquake, much of the refinery was shut down for an annual inspection. Damage to the refinery and lost oil represent one of the major losses in this earthquake (Ellingwood, 1980).

The subsequent shutdown of the refinery rendered the adjacent oil-fired New Sendai Power Plant inoperable for lack of fuel (Ellingwood, 1980). In addition, the power plant, owned and operated by the Tohoku Electric Power Company, suffered damage to both boilers. The plant was shut down for 6 days for repairs. Total damage to Tohoku Electric Power Company facilities was \$15 million, 10 percent of which was at the New Sendai Power Plant (EERI, 1978).

The Sendai City Gas Bureau reported the total collapse of a large telescoping propane gas holder at its Haranomachi plant. The gas holder held 14,000 cubic meters of propane gas at low pressure. The collapsed tank caught fire shortly after the failure and all of the stored gas was consumed (a total of 10 fires were started as a result of this earthquake). The fire burned for 25 minutes, but did not spread to nearby high pressure propane tanks (Ellingwood, 1980). However, the collapsing tank struck a nearby pipeway, causing additional damage to piping systems and other associated equipment. The collapse and the resulting damage to gas mains were the primary cause of service interruption and shutdown of the electrical generating plant in North Sendai (EERI, 1978). The natural gas and resulting electricity outage interfered with medical services, but no overloading of hospitals was reported.

Damage to the natural gas distribution system in Miyagi Prefecture was a major recovery problem. Low pressure gas distribution systems in 6 cities were severely affected and restoration required more than three weeks. The Sendai City Bureau of Gas serves 136,000 customers with 1,741 kilometers of buried lines. There were 4 minor failures in medium pressure transmission lines. Low pressure distribution pipes were extensively damaged, with over 550 failures identified. After four weeks, all restorable meters were returned to service. The total cost of restoration was ¥850 million (Ellingwood, 1978).

### **1971 San Fernando Valley (M = 6.6)**

Damage to natural gas transmission pipelines was extensive and concentrated in areas of ground failure - lateral spreading, liquefaction-induced landslide and surface faulting. The failure of several 1925-1930 vintage oxyacetylene welded steel transmission pipelines resulted in serious disruption of gas service, as these lines bring gas from the San Joaquin Valley through the Newhall Pass to the Los Angeles Basin (Johnson, 1983).

Damaged lines between Newhall and San Fernando had to be shut down, resulting in loss of supply to a 12 square mile area with 17,000 customers.

Two Southern California Gas Company transmission pipelines (lines 85 and 100) as well as one Getty Oil Company pipeline located in the area of lateral spreading and liquefaction-induced landslides near the Upper Van Norman Reservoir were damaged. In the area of lateral spreading, movements were as large as 1.7 meters. Line 85 was repaired at 7 locations within the lateral spread (O'Rourke and Tawfik, 1983). Two of these repairs were at sites of explosion craters, three to four meters in diameter, formed by the sudden release of high pressure gases.

Line 1001 had multiple breaks and was subsequently abandoned. Within the area of liquefaction-induced landslides, the Getty oil pipeline failed in tension. Another high pressure natural gas transmission line (line 115) was located within the zone of surface faulting for this event. Line 115 crossed the Sylmar segment of the fault, and passed through areas of both compressive and tensile ground movement. In the area of compressive ground movement, the pipeline was subject to beam buckling, compressive wrinkling, shortening and rupture. In areas of tensile ground movement, explosion craters, typically three meters in diameter, appeared at several locations (McCaffrey and O'Rourke, 1983). One fire was caused by escaping gas. (There were 11 explosion craters caused by rupture of line 115 within one km of the Sylmar segment of the San Fernando Fault Zone).

The cost for repair of the transmission facilities was approximately \$232,000. Repairs made in the San Fernando area were as follows (McNorgan, 1973):

- 53 breaks in line 115 (16")
- 9 breaks in line 85 (26")
- 8 breaks in line 1001 (12") - 5 miles of this line were abandoned

- 3 breaks in line 102 (12")
- 1 break in line 104 (10")
- 1 break in line 119 (22")
- 1 break in line 120 (22")

The natural gas distribution system also experienced damage. The most serious damage was in an area of 12 square miles that suffered 380 breaks (181) main breaks, 137 service breaks, and 62 breaks in service to main connections. Fifty thousand feet of damaged pipe were replaced. Repair and restoration cost approximately \$1.5 million and took 12 days.

### **1964 Alaska (M = 8.4)**

The Great Alaska Earthquake is the largest magnitude earthquake studied, and the losses from this event were extensive. Damage, documented by the National Academy of Sciences (NAS, 1973), was dispersed throughout several communities.

In Whittier, Alaska, damage to Union Oil Company tanks resulted in the release of combustible liquids and a fire that burned for three days. Over five million gallons of various types of fuels were destroyed, along with 472 barrels of refined products. All 11 tanks at the facility were ruptured, and only three remained standing. At the adjacent US Army Petroleum Distribution Facility, 56,000 barrels of diesel fuel were lost from tank rupture, fire (which started at the Union Oil Co. facility) and draining of four 12 in. diameter lines. Three thousand barrels of jet fuel were lost from a leak in a pressure relief pipe.

A total of seven tanks in Anchorage containing combustible fluids collapsed and released their contents. Three Standard Oil tanks at the Anchorage airport released 750,000 gallons of aviation fuel. In the dock area, two Standard Oil Company 100,000 gallon tanks leaked 50,000 gallons of gasoline. Precautionary measures taken for the natural gas distribution system in Anchorage paid off. Gas pressure-regulating valves, which close when there is a large pressure drop on either side, had been installed on almost all service connections by the Anchorage Natural Gas Company. During the earthquake, these valves closed when the street mains or any of the interior gas lines were broken.

At Seward, fuel storage tanks at the petroleum tank farms along the waterfront (Standard Oil Co. and Texaco) ruptured, leaking fuel into the bay. The fuel caught fire and tsunamis spread blazing gasoline and oil over parts of the city. The Union Oil Company tank farm in Valdez

was destroyed when fire broke out in fuel-oil storage tanks at the waterfront.

**1964 Niigata, Japan (M = 7.5)**

Fire damage was severe in this earthquake. At the Niigata Refinery, crude oil from a tank ignited and the fire burned for four days, destroying 64 buildings, 149 out of 169 tanks, and causing the loss of 201,000 kl of oil. Explosion and fire also caused damage at the old Showa Oil Refinery. Damage to the two facilities totaled ¥4.6 billion. Fires also burned at the Narusawa Mineral Oil Company and the Nihon Oil Co.

Buried gas pipelines were severely damaged by ground slippage induced by liquefaction of sandy soil. Break rates were calculated for the 131 km of cast iron pipeline; 51 joint separations occurred (0.4 per km) as well as 80 main breaks (0.6 per km). Along the 17 km of welded steel line, there were 13 breaks (0.8 per km).

## SECTION 3

### COMPONENT FRAGILITY MODELS

#### FUNCTIONAL HIERARCHY

The ensuing system analysis requires the identification of the functional hierarchy of the components of an oil transmission in the form of a fault tree. Figure 1 shows a fault tree representing the interrelationship among the components of a simplified oil transmission system. It shows, in accordance with the definition of "and" gate, that the seismic performance of this transmission system depends on the performance of four "major" component facilities consisting, in this case, of two pumping stations, pipeline network, and a control building, contributing directly to the system performance. Although examples of "or" gates do not appear in Figure 1, they exist in the full fault tree for the system and used in the systems analysis. Figure 1 further shows that these four components can in turn have their own contributing components. For example, a pumping station has three such contributing components. This process of breaking down a component continues until it reaches either a "basic" component that can no longer be broken down to contributing components, or a "component facility" consisting of a set of constituent components which function and resist seismic effects in combination as a unit (e.g., pumping station building). For brevity of writing, no distinction will be made between basic components and component facilities in the following as long as no confusion arises.

#### COMPONENT FRAGILITY

In performing a systems analysis, the fundamental probabilistic unit is the fragility curve which represents the probability  $P_i(x)$  that a basic component  $i$  will not be functional at a specified level of functionality when it is subjected to the seismically induced ground or support motion with intensity  $x$ . The intensity of support motion may be measured by translational and/or rotational (peak or spectral) acceleration, velocity or displacement (or relative displacements between multiple supports). The fragility of the underground pipeline network is characterized, however, by the rate (per unit length) of pipe failure along the pipe as the parameter of the Poisson process model. This rate depends on the material, diameter, and age of pipe, joint configuration, soil condition, and the ground motion intensity, among possible others. Rigorously speaking, fragility of pipe failure also depends on the specified level of oil leakage associated with the pipe failure. Hence, a family of fragility curves emerge as shown in

Figure 2 where the curve signified by  $P_i(x, \text{minor})$  indicates the probability that the basic component will suffer from at least minor level of damage/malfunction (or oil leakage in case of pipe failure) when it is subjected to ground motion intensity  $x$ . Similar definitions apply to two other curves signified by  $P_i(x, \text{moderate})$  and  $P_i(x, \text{major})$ . For a prescribed support motion intensity  $x$ , therefore, probabilities with which minimal, minor, moderate and severe levels of damage/malfunction will occur are specified for each basic component by this family of fragility curves. Obviously, this makes it a straightforward task to generate, by the Monte Carlo method, sample values of the degree of damage/malfunction of each basic component under a prescribed value of ground motion intensity. The category of degree/malfunction does not have to be confined to the four levels considered above, depending on the details of available damage/malfunction information.

Fragility of a component consisting of a number of constituent basic components must also be evaluated by means of Monte Carlo techniques. Referring to Figure 1, for example, the pumping station, one of the four major components of this hypothetical oil transmission system, consists of three constituent components; a pump, connecting pipes and a station building each of which is considered as a basic component in this study. A set of three realizations of damage/malfunction level for these basic components simulated by the Monte Carlo method are used to evaluate the level of damage/malfunction of the pumping station under the scenario earthquake. This process of evaluating the level of damage/malfunction is repeated as many times as needed under the scenario earthquake with different magnitude in order to establish a family of fragility curves for this major component. Families of fragility curves for other three major components; another pumping station at a different location, pipeline network for the entire system and a control building, can be similarly established using the Monte Carlo method under the same scenario earthquake.

Efforts are made in the following to examine the database available in ATC-13 (Applied Technology Council, 1988) and ATC-25 (Applied Technology Council, 1991) which are based primarily on the collective professional experience and judgement.

ATC-13 developed earthquake damage and loss data on the basis of the experience and judgment of seasoned earthquake engineers. Direct damage from ground shaking, for example, is presented for 78 earthquake engineering facility classes including various types of buildings, bridges, pipelines, dams, tunnels, storage tanks, roadways and pavements, chimneys, cranes,

conveyor systems, towers, other structures (canals, earth retaining structures, waterfront structures) and equipment. The data are summarized in the form of DPM (damage probability matrix) which is equivalent to the family of fragility curves introduced above. DPM's developed in ATC-13 for the 78 facility cases use "central damage factor" (CDF) to categorize the level of damage, instead of more qualitative designations such as "minimal", "minor", "moderate" and "severe". CDF represents the level of damage in terms of the average value of ratio of repair cost to replacement cost. Table 4 shows such a DPM for a class of low-rise reinforced concrete shear-wall buildings with moment-resisting frame. Compared with the family of fragility curves considered in Figure 2 in which the probability values are associated with a specific support motion intensity measured in gal, MMI (Modified Mercalli Intensity) is used for DPM to indicate the ground motion intensity. DPM can be derived from the fragility curves, however. In the case of Figure 2, appropriate conversion of support (ground) motion intensity to MMI transforms the ground intensity scale to MMI and average probability values for various damage levels associated with corresponding MMI can be read. This makes it possible to develop a DPM corresponding to the family of fragility curves. ATC-13 also provides database for direct damage from collateral hazards. ATC's damage database for the earthquake engineering facilities pertinent to oil transmission lifelines such as pipelines, storage tanks and equipment are useful for a preliminary and first approximation analysis.

ATC-25 develops, on the basis of the same methodology and assumptions as used in ATC-13, lifeline vulnerability functions which describe fragility curves for essential components and proposes restoration curves for lifeline systems. While ATC-13 was primarily developed for California structures, ATC-25 database is applicable to the facilities, components and systems located elsewhere. In this context, reference is made to NEHRP Seismic Map Areas replotted in Figure 3 from BSSC, 1988. In the figures where example fragility and restoration curves will be shown, specific mention is made to identify the areas in which these curves are valid. Direct quote from the ATC-25 (p. 26) with respect to these areas is given below.

- a. California NEHRP Map Area 7 (CA 7), which we take to be the only area of the United States with a significant history of lifeline seismic design for great earthquakes,

- b. California NEHRP Map Areas 3-6 (CA 3-6), Non-California Map Area 7 (Non.CA 7; parts of Alaska, Nevada, Idaho, Montana and Wyoming), and Puget Sound NEHRP Map Area 5 (P.S.5) which we take to be the only regions of the United States with a significant history of lifeline seismic design for major (as opposed to great) earthquakes, and
  
- c. All other parts of the United States (other), which we assume have not had a significant history of lifeline seismic design for major earthquakes.

Typical fragility curves and restoration curves for petroleum fuels distribution storage tanks are copied directly from ATC-25 (pp. 286-297) in Figure 4 and Figures 5-7, respectively for illustration purposes. For the same purpose, the restoration curve for a crude oil delivery system is shown in Figure 8, again taken from ATC-25 (p.390). ATC-25 contains damage and restoration database that are useful for a preliminary systems analysis of lifeline systems. However, the type of systems analysis that involves flow analysis of liquid medium in damaged lifeline systems as will be discussed in the following section was not considered in ATC-25. Nor was consideration given to the environmental contamination potential arising from the leakage of the fluid from the locations of pipe failure. The contamination containment and remediation entail significant amount of cost which may far exceed the cost of repairing the damaged facilities. Cost associated with the contamination has not been studied extensively in spite of the fact that it can be a dominant cost component. This is the reason for this study to have a section (Section 6) dedicated to this subject matter. The result of the NIBS/FEMA loss estimation study has not been made public as yet, and therefore no review has been possible.

## SECTION 4 SYSTEM FRAGILITY MODELS

### SYSTEMS ANALYSIS

Functionality of spatially extended and complex lifeline systems cannot be evaluated probabilistically by straightforward analytical manipulation on the fault tree utilizing fragility curves of constituent components. The systems analysis must be performed with the aid of Monte Carlo techniques in order to simulate the physical damage the system sustained and resulting system malfunction under the scenario earthquake. This is the significance of the entry "systems analysis" in Figure 1. The reason for this stems from the fact that the definition of the functionality of a lifeline system transporting liquid medium is quite complex. The functionality for such a lifeline system involves at least two factors.

The first relates to the system functionality immediately after an earthquake involving the pressure and flow rate at demand nodes. After an earthquake, the system may be defined functional if the aggregate (or average) flow rate having an acceptable level of medium pressure with respect to all the demand nodes remains above, say, 80% of the corresponding value of the system before the earthquake. On the other hand, the system may be considered functional, when only a few but selected critical demand nodes (e.g., supplying the transported material for key regional industries) continue to provide a sufficient level of pressure and flow rate performance. A more practical definition of the functionality, however, must prudently combine these two requirements. Furthermore, the extent of system performance degradation will be quite different depending on a particular set of components sustaining seismic damage of varying degrees under each scenario earthquake even with the same magnitude.

In fact, extensive research was carried out on the seismic performance of lifeline systems including MLGW's (Memphis Light Gas Water's) water, gas and electric power systems, Southern California Gas Company's system, LADWP's (Los Angeles Department of Water and Power's) water and electric power systems, and the San Francisco's AWSS (auxiliary water supply system). In all these cases, the system performance is estimated probabilistically with extensive use of Monte Carlo simulation techniques by taking advantage of the component fragility information.

The result of the seismic performance analysis mentioned above has also been utilized in the

estimation of direct and indirect economic impacts, particularly in relation to the seismically induced service interruption of MLGW's lifeline systems (e.g. Chang et al., 1995a, Chang, et al., 1995b, Rose, et al. (forthcoming), Rose, et al. 1995). In doing so, economic losses incurred by the utility company itself, as well as various industry sectors within and outside the seismically impacted region, have been estimated.

Within the general framework of the Monte Carlo simulation approach mentioned above, a methodology must be developed in order to evaluate the cost-effectiveness of the design code upgrading and seismic retrofit. For this purpose, on the one hand, knowledge is required of the cost of implementing the upgraded guidelines in constructing new structures and of executing the seismic retrofit on existing structures. On the other hand, the benefit that these implementations will bring must be evaluated. Acquiring such knowledge and evaluating the benefit of implementation constitute an important task. The experience of the 1994 Northridge and the 1995 Hyogoken Nanbu (Kobe) earthquakes showed that both implementation of upgraded design codes and execution of the seismic retrofit significantly improved the seismic performance of the structures. Cost and benefit data must be sought from the experience of these and other earthquakes.

The second factor relates to the restoration of the system in which the time required to restore the damaged system becomes the crucial quantity. In view of the past experience, the restoration of utility service is one of the most urgent post-earthquake tasks to be accomplished by responsible utilities as fast as possible. The process of this restoration is depicted by a restoration curve in Figure 9a, where the restoration is measured in terms of the ratio of the supply of utility service to the demand that exists as a function of the elapsed time after the earthquake. For the purpose of estimating direct and indirect cost due to an earthquake with magnitude  $m$ , the restoration curve plays a crucial role. In Figure 9a, curves (a), (b), (c) and (d) respectively depict, in an idealized manner, the rate of increasing slower restoration in response to severer states of post-earthquake system damage. Figure 9b shows actual restoration curves for water delivery systems in Japan and California following a number of different earthquakes.

*It is of great importance to reiterate here that, for this purpose, the Monte Carlo simulation of the state of system damage based only on the fragility curves of the major components is not sufficient. In this case, the application of the Monte Carlo simulation is necessary starting with the basic components, so that each state of system damage can be identified as a specific set of damaged (or malfunctioning) basic components leading to the system degradation*

*requiring repair to restore the system function on an emergency basis.*

This knowledge of damaged basic components permits one to develop a corresponding restoration curve for each state of simulated system damage under an earthquake with magnitude  $m$ . Based on the experience on the part of the authors of this report, a sample size of 20 to 50 for the Monte Carlo simulations at each level of earthquake magnitude is considered reasonable. As just mentioned, each sample state of damage, in principle, results in a corresponding unique restoration curve. This is for the reason that each state involves a different set of damaged or malfunctioning components, and the restoration effort depends on the number of such components, their types and the nature of the physical damage sustained by them. For the same reason, each restoration curve is associated with a differing level of economic loss, direct and indirect combined. Hence, the economic loss  $L$  is probabilistic even though the system is subjected to scenario earthquakes of the same magnitude;  $L$  depends on a particular realization  $i$  and at the same time is also a function of the magnitude  $m$  of the scenario earthquakes, i.e.  $L=L_i(m)$ .

Total recovery and possible seismic and non-seismic upgrading of the system will usually follow the emergency repair and restoration, and probably entail significant longer-term expenditures. The part of these expenditures specifically pertaining to the system restoration may be considered direct cost of the earthquake.

## SOCIO-ECONOMIC LOSS AND SYSTEM FRAGILITY

Socio-economic losses corresponding to restoration curves including direct and indirect losses must be evaluated based on damage sustained and services interrupted. In doing so, first consider seismic hazard function  $H(m)$  for the scenario earthquake as shown in Figure 10, where  $H(m)$  is simply the normalized conditional probability version of the Gutenberg-Richter relationship for a specific seismic zone, and  $m$  denotes the magnitude between upper and lower bounds  $m_u$  and  $m_l$ . It is conditional to the event that an earthquake with magnitude  $m_l \leq m \leq m_u$  has occurred. This event has an expected number of annual occurrences ( $N_0/\text{yr}$ ) depending on the regional seismicity and on the value of  $m_l$  below which the earthquake is considered engineering-wise insignificant.

The expected value  $\bar{L}(m)$  of  $L_i(m)$  over the sample of size  $N$

$$\bar{L}(m) = \frac{1}{N} \sum_{i=1}^N L_i(m) \quad (1)$$

will be used to estimate *the expected conditional economic loss*  $\bar{L}(m)$  of the system given the scenario earthquake with magnitude  $m$ . In Figure 10,  $\bar{L}(m)$  is schematically drawn using an arbitrary unit. *Then,  $\bar{L}(m)$  serves as the system fragility curve.* For a specific lifeline system, it may not be very difficult to develop a family of fragility curves, from the simulated ensemble of  $L_i(m)$  ( $i=1,2,\dots,N$ ) particularly when  $N$  is large, which represent minimal, minor, moderate and major levels of economic loss. In the present study, however the expected conditional economic loss  $\bar{L}(m)$  will be conveniently used for the ensuing economic analysis and therefore "a family of fragility curves" are not developed from the ensemble of  $L_i(m)$ . This issue will be revisited when the result shown in Figure 10 is discussed in Section 6. This fragility curve is then combined with the conditional density function  $h(m)$  of the magnitude  $m$  of the scenario earthquake to produce  $L^*$  as below.

$$L^* = N_o \int h(m) \bar{L}(m) dm \quad (2)$$

where  $L^*$  gives the *expected annual economic loss* sustained by this system under earthquakes with any magnitude, where  $h(m)$  is equal to  $-dH(m)/dm$  as shown schematically in Figure 10 (scale is relative for  $h(m)$ ).

In the ensuing economic analysis, the following assumptions are made for the ease of demonstration of the methodology; (a) the occurrence of the scenario earthquake is statistically independent each year, (b) all the direct and indirect losses resulting from a scenario earthquake are incurred in the year of its occurrence: long-term future reconstruction cost must carefully be evaluated and converted to the present worth value at the same year in this model, which may need improvement in the future, and (c) the present worth PWL of the loss is computed over the specified life of the lifeline with  $L^*$  representing the annual loss each year. The value of discount rate will be treated as a parameter in this economic analysis.

## BENEFIT-COST ANALYSIS

The costs of implementing the reference design guidelines and its upgraded version are denoted by  $CD$  and  $CD+\Delta CD$ , respectively. The present worth of the losses associated with the system designed under the reference and upgraded guidelines are written as  $PWL_0$  and  $PWL$ , respectively. The sum of  $PWL$  and the cost differential of the guideline implementation  $\Delta CD$  is plotted as a function of  $\Delta CD$  in Figure 11. The optimal level of design guideline upgrading is identified as the level at which the cost differential ( $\Delta CD_{opt}$ ) corresponds to the minimum value of  $PWL+\Delta CD$  as shown in Figure 11.

Determination of the  $PWL$  curve and the associated optimal level of  $\Delta CD$  will depend upon the context of the problem. If the optimal level of design is being pursued from the narrow standpoint of utility company investments, then the relevant economic losses (reflected in  $PWL$ ) may consist of expected repair costs and loss of utility revenues resulting from damage and service disruption. If pursued from a broader societal standpoint, both direct business interruption losses to the utility customers and downstream (indirect) economic losses should also be considered.

In the case of seismic retrofit, however, the effect and the cost of retrofit depend on which basic components receive retrofit and to what extent. The present worth  $PWL$  of the annual expected loss is a function of the cost  $\Delta CR$  of retrofitting the basic components designated under each specific retrofit strategy. In some cases, the retrofit strategy includes enhancement of redundancy (for example, adding a new pipeline route to a network of the existing pipelines) and replacement of some basic components. The sum of  $PWL$  and the cost  $\Delta CR$  associated with each retrofit strategy is plotted as a function of  $\Delta CR$  as shown in Figure 12. In this case, strategy 1 provides the optimal retrofit cost  $\Delta CR_{opt}$ .

## ACCEPTABLE LOSS

In practice however, the optimality should be determined under the acceptable loss criterion as shown in Figures 11 and 12. This is because the determination of an "optimal" level of design or retrofit will typically also involve factors external to the cost-minimization problem. They may include such factors as risk adversity or politically acceptable levels of public safety. When these external factors are taken into account, the acceptable point may be shifted in either direction. This can be represented by introducing an "acceptable loss level" as shown in Figures

11 and 12. In Figure 11, the acceptable level of economic loss is achieved by spending the optimal cost differential  $\Delta CD_o$  rather than  $\Delta CD_{opt}$  associated with the global optimal value. A similar relationship exists between  $\Delta CR_o$  and  $\Delta CR_{opt}$  as shown in Figure 12. Without attempting to identify a unique level of "acceptable loss" for evaluation, it is nonetheless very useful to examine the cost and loss implications of different possible realizations of "acceptable loss" in the development of the conceptual framework for determining design and retrofit guidelines. The flow charts of actions required for finding  $\Delta CD_o$  and  $\Delta CR_o$  are respectively shown in Figures 13 and 14. In fact, these figures also schematically describe the framework for the development of design and retrofit guidelines, which will be described in detail in Chapter 6.

*The analysis above is performed under a specific scenario earthquake at a given epicentral location with probabilistic variability in magnitude. The Gutenberg-Richter relationship is introduced in Figure 10 and interpreted as the seismic hazard for the region surrounding the epicenter. This is the correct interpretation if the scenario earthquake under consideration is the only earthquake to be concerned. The lifeline risk assessment involving seismic hazard represented by area or line source or its mixture still requires the scenario earthquake-based probabilistic analysis. This can be done by (1) dividing the area or line source into small areas or line elements with the corresponding Gutenberg-Richter relationships properly adjusted, (2) utilizing the same method of analysis described above for the evaluation of expected loss  $L(m)$  for each area element, and (3) further taking the expected value of  $L^*$  with respect to all the area elements, and eventually taking the expected value of  $L^*$  thus obtained for all the areas. This process makes the analysis highly cumbersome without adding much to the understanding of the framework to be developed for design and retrofit guideline development. For this reason, this report considers a framework for design and retrofit framework under a scenario earthquake with a fixed epicenter with a probabilistic magnitude.*

## **SECTION 5**

### **SEISMIC DESIGN AND RETROFIT GUIDELINES**

Framework for seismic design and retrofit guidelines for lifeline systems in general is developed in this chapter with the understanding that uncertainty and reliability allocation issues must be carefully addressed as indicated below.

#### **UNCERTAINTY ANALYSIS**

Fragility and restoration curves discussed above do contain a possibly significant amount of uncertainty originating from a number of sources. Among the important sources, the attenuation law, the intensity of support (or ground) motion and the limit states of the components for which the fragility curves are to be developed appear to be the most dominant. Within the framework of probabilistic systems analysis, the uncertainty associated with these and other sources is estimated in terms of a confidence band on the empirical basis complemented by analytical and experimental studies as much as possible. This leads to the concept of an engineering confidence band centered around the fragility curve developed on the basis of the "best estimate" as schematically illustrated in Figure 15. More importantly, each of the resulting restoration curves, which are distinct from each other due to the sample variability in the Monte Carlo simulation of the system damage state, will have its own confidence band arising from the various sources of uncertainty. The combined confidence band for the restoration curves must be estimated accordingly, which in turn determines the confidence interval for the total economic loss estimation. The uncertainty propagates through each layer of the hierarchical structure of components and may produce possibly a wide confidence interval for the total annual expected economic loss estimation. Computationally, however, present-day computer capability makes it easy to establish an order-of-magnitude estimation of the confidence interval.

#### **RELIABILITY ALLOCATION**

The forward probabilistic systems analysis starting with the basic components to estimate the total annual expected economic loss tends to be complex, requiring Monte Carlo techniques as elaborated in the preceding discussion. From the viewpoint of the development of the design or

retrofit guidelines, however, even more complex inverse analysis that can determine the degree of adjustment of each fragility curve, or equivalently reallocate the reliability to each of the basic components is required. Indeed, only through this inverse process of reliability allocation, can a fragility performance level or a target level of reliability be assigned to each basic component or component facility, and its design upgrading and retrofit improvement can be pursued to attain that target level. Rigorously speaking, the inverse analysis is not possible because of the unavailability of unique solutions. *Practical solutions will be obtained, however, on the basis of iterative applications of the forward analysis that will identify critical components with significant contributions to the total economic loss. With the aid of contemporary computational capability, this is not a very difficult task. A similar problem was dealt with in a nuclear power plant PRA.*

#### FRAMEWORK FOR PROTOTYPE DESIGN AND RETROFIT GUIDELINES

The procedural framework for the development of design and retrofit guidelines is illustrated in Figures 13 and 14, respectively. In order to implement, for example, the acceptable loss-based guidelines in the format of conventional design, Figure 13 considers the use of existing design guidelines for all the basic components. This is done in the same spirit as the LRFD specifications are given in the conventional format, although it is firmly based on structural reliability principles. If such guidelines do not officially exist for some of the basic components, conventional design procedures currently in practice can be used as a starting point.

Fragility curves will then be estimated for the basic components thus designed. Making use of these fragility curves, systems analysis will be performed next in order to generate restoration curves. This permits the economic analysis to be carried out in Monte Carlo simulation for the evaluation of the present worth of economic loss  $PWL_0$ , as defined in Chapter 4. If  $PWL_0$ , so evaluated is below the threshold acceptable level, the design guidelines used at the start of this exercise is indeed also acceptable. If, however,  $PWL_0$  is not below the threshold and hence the initial guidelines are not acceptable, the process of reliability reallocation or selective fragility enhancement as introduced above must be executed. Through this iterative process, the "critical" basic components will be identified whose fragilities can be most cost-effectively enhanced, and the design guidelines will be upgraded accordingly. This will result in the reduction of present worth of economic loss from  $PWL_0$  to the threshold acceptable level at the expense of the cost differential equal to  $\Delta CD_0$ , if the iteration brings the economic loss to the designated threshold acceptable value.

A similar procedural framework is illustrated in Figure 14 in the form of a flow chart for retrofit procedures. Here again, however, the "critical" basic components and component facilities should be identified first by carrying out the forward systems analysis and retrofitting be implemented for them to enhance their fragilities.

**BLANK PAGE**

## SECTION 6

### AN EXAMPLE OF ECONOMIC LOSS

The objective of this section is to demonstrate how conditional economic loss  $L(m)$  can be estimated dealing with the cost of environmental contamination arising from oil spill out of seismically induced pipe failures. While the pipelines and earthquake scenario analyzed are of technical and social interest, the scope of the chapter permits only a limited view of the analysis. For a more complete description of the methodology, the reader is referred to Pelmulder et al. 1997. The two pipelines studied were Mobil line number 68 and the Capline System operated by Shell. These are major pipelines which move crude oil from Texas and the Gulf Region to refineries in the Midwest. The pipelines were analytically subjected to ground shaking equivalent to a magnitude 8.6 earthquake located along the New Madrid Fault Zone.

The earthquake hazards will first be described, followed by the pipeline model. Finally, the application of a library of environmental models will be discussed and the results presented.

#### HAZARD DATA

The earthquake scenario selected for this study was a magnitude 8.6 event located along the New Madrid Seismic Zone (NMSZ). Modified Mercalli Intensity isoseismals for this scenario were mapped by Algermissen and Hopper (1984). This scenario is equivalent to a single earthquake with a very long rupture length or a combination of large events, such as the 1811-1812 series of earthquakes. If a single event occurs, the contour near the epicenter may extend too far north or south. However, as Algermissen and Hopper point out (Hopper, pg. 49) "cities far away from the zone would experience about the intensities shown, no matter which section of the seismic zone the earthquake occurred."

A single event of this magnitude ( $M_s \geq 8.3$ ) is estimated to have a return period of 550 ( $\pm 225$ ) years and a 0.003-0.01 probability of occurrence by the year 2000 (Johnston and Nava, 1985). While the probability will have changed somewhat in the last 7 years, it will be assumed for this example that the probability of the magnitude 8.6 event mapped by Algermissen and Hopper is 0.005 within the next 25 years.

Another significant seismic hazard is liquefaction-induced ground failure. In general, four types of ground failure result from liquefaction (Youd, et al. 1978); lateral spreading (resulting in

horizontal and vertical movements of the ground), flow failure, ground oscillation, and loss of bearing strength. Areas of moderate to high liquefaction potential were mapped by Obermeier (1985) for seven states in the Central U.S. Only areas within the MMI IX isoseismal of the Algermissen and Hopper map were identified.

No distinction was made on the Obermeier maps between areas of liquefaction and landslide, or areas of greater and lesser potential. While it is possible to overlay liquefaction potential with slope to delineate areas of landslide from liquefaction, doing so was beyond the scope of this study. Further, it is necessary to assign a probability that liquefaction will actually occur at a particular location, given that it is in an area of potential liquefaction. This probability depends on both the NIMI at the location and the magnitude of the event. Larger MMIs contribute to larger shear stresses in the soil during each oscillation, while larger magnitudes generally increase the duration of strong ground motion and lead to larger numbers of oscillations in which to build up pore pressure. Based on the description of areas mapped by Obermeier (1985), an average liquefaction probability of 37.5 percent in areas of MMI IX-X was estimated for this scenario.

Both the MMI and liquefaction potential maps were digitized and processed using a Geographic Information System (GIS). Figure 16 shows the digitized MMI map overlain with state boundaries, while liquefaction potential is shown in Figure 17.

## PIPELINE MODEL

The pipelines selected for this study were Mobil line number 68 and the Shell Capline. The routes of these pipelines are shown in Figure 18. The Capline pipeline is 40 inches in diameter and was built in 1968 from API 5LX-X52 grade welded steel pipe with arc welded joints (Ariman et al., 1990). Line 68 is 18 and 20 inches in diameter and was built around 1948 of Grade B steel with welded joints.

The Capline was analyzed from Liberty, Mississippi to Patoka, Illinois, while line 68 was studied from Lanespport, Arkansas to Joliet, Illinois. The pipeline routes were laid out on 1:24000 and 1:62500 scale USGS topological maps. In areas where the exact route was unknown, a straight line route between pump stations was assumed. Block valves were assumed to be located at pump stations, on either side of rivers and other surface water greater than 100 feet wide at the crossing, and approximately every 14 miles. Elements were selected

such that the basic topography was maintained.

A summary of the exposure of these pipelines to a magnitude 8.6 event on the NMSZ is provided in Table 5. While line 68 has a slightly larger exposure to NM VII or greater, the Capline has a significantly greater length of pipe exposed to potential liquefaction. Since line 68 is generally more vulnerable than the Capline, due to its age and construction, it may be expected to experience more leaks, even though it is exposed to a lower overall hazard level.

#### APPLICATION OF LIBRARY MODELS

An appropriate environmental model was assigned to each element based on its proximity to surface water, wetlands and floodways, and the general terrain.

The five models considered in this study are:

1. Leaks occurring away from rivers and flood plains- Moderate terrain (Model 1).
2. Leaks occurring away from rivers and flood plains - Hilly terrain (Model 2).
3. Leaks occurring away from rivers, however, in flood plains or wetlands (Model 3).
4. Leaks occurring under a river with deep cover (Model 4).
5. Leaks occurring under a river with shallow cover (Model 5).

A more detailed description of these models including their mathematical formulation is contained in Pelmulder et al. 1997.

Values for depth of water table were generalized from U.S. Department of Agriculture Soil Surveys and Water Resources Maps. The remediation cost schedule for all models is contained in Table 6.

The values in Table 6 were used to determine the expected cost for each model scenario over a range of spill volumes. The models were evaluated at 50, 150, 250,...60,000 bbl. The costs associated with the various volumes were stored in an array to be used by the simulation routine. Figure 19 contains plots of expected cost vs. volume for models 1, 2, and 3, while Figure 20 contains that for model 5. Model 4 does not depend on volume because the flow is

restricted by the soil and rock. It should be noted here that these cost curves, although based on the estimates of experts in the field, represent preliminary values and must be viewed as such. In general, though, the costs associated with surface water remediation are significantly higher than those associated with soil or groundwater remediation.

The expected costs for each range of spill volumes were derived from the discrete distributions of costs obtained from the event trees and stored in a data array to be used by the simulation routine. When the oil release model returned a value between 0 and 100 bbl, the cost associated with 50 bbl was used. It is possible to linearly interpolate between the evaluated volumes to obtain a better approximation of the cost; however the difference in cost is not significant enough to warrant the extra computation time.

The range of costs possible for a given volume and model is shown in Figure 21 which contains the frequency of exceedance curve for a 1000 bbl spill in a model I type area. The stars indicate the discrete values which the model calculated. There are several values from three to six hundred thousand dollars. Because there are also several branches of the event tree which produce each of these costs, the frequency of exceeding three hundred thousand dollars is 0.25. In each of these cases, there has been large scale groundwater contamination. Approximately half of the remaining branches of the event tree have costs of about fifty thousand dollars. These costs correspond to small scale groundwater contamination and various degrees of soil contamination. When there is soil contamination only, the cost ranges from two to twenty thousand dollars.

## RESULTS

The simulation of the NMSZ magnitude 8.6 earthquake was performed with 200 thousand trials representing 200 thousand possible outcomes given this type of event. This large number of trials was used for illustrative purposes so that discontinuities in the loss curves are due to physical phenomena. Essentially the same numerical results could have been obtained with 25-50 thousand trials. The results obtained from this simulation include the risk of direct physical damage to the pipeline and risk to the environment from oil spills.

The risk of pipeline damage is expressed as frequency of exceedance of number of failures and is shown in Figure 22. Each failure is an element requiring repair. The maximum frequency is 1.0 because this is a conditional curve, i.e., exceedance frequencies given that the event has

occurred. While it is theoretically possible to have a simulation trial in which no leaks occur, the probability of failure for this system in this event is high enough that the minimum number of failures in this simulation was 20. At the high end of the scale, in two trials the number of failures exceeded 500. These are the extreme cases. When the frequency of each number of failures is considered, the expected number of failures given this event is 87. It is worthwhile to note that the extreme maximum is more than four orders of magnitude less likely to occur than the expected value.

In this study, a constant value of \$5,000 has been assumed for each pipeline repair. Therefore, the horizontal axis of Figure 22 can be multiplied by \$5,000 to obtain the frequency of exceedance for cost of direct damage. In this case, the minimum direct damage loss is \$100,000, the maximum is \$2,500,000, and the expected direct damage loss is \$435,000.

The losses for a region are the sum of losses from many single locations. It is, therefore, useful to examine the distributions of losses at single sites to understand how the simulation and models affect the results. While it is possible to choose an element and keep track of the distribution of volumes or dollar losses at this location, what is of interest here is the distribution of all single site losses which occur in the system during the simulation. Single site losses are also the curves used when operational failures are modeled, as these are assumed to occur one at a time.

The conditional frequency of exceedance of spill volume at a single location is shown in Figure 23. This is also known as a cumulative distribution and has been normalized by the total number of spills so that the maximum exceedance frequency is 1.0. The minimum spill volume is 50 bbl, the maximum is 60,000 bbl, and the expected value is 4700 bbl. Again, the maximum value is at least four orders of magnitude less likely to occur than the expected value. Of particular interest in this figure is the change in slope at approximately 12,000 bbl. A spill of this volume is about equally likely to occur on line 68 as it is on the Capline. Spill volumes less than 12,000 are more likely to occur on the 18-20 inch diameter line 68, while volumes greater than this are more likely to occur on the 40-inch diameter Capline.

Because each pipeline element is allowed to fail independently, the single site spill volume exceedance curve can be thought of as the sum of curves for each pipeline. Since line 68 is significantly more vulnerable than the Capline, if a leak occurs, it is likely to be on line 68. The frequency of exceedance curve for line 68 alone, then starts near 1.0 at 0 bbl, following

approximately the curve for the combined system until around 12,000 bbl. Since the maximum spill volume for line 68 in the simulation was approximately 25,000 bbl, the curve for line 68 has declined to zero by this point. In contrast, the curve for the Capline alone would have an exceedance frequency of less than 0.1 at 0 bbl. After approximately 12,000 bbl, the Capline curve would be close to, and after 25,000 bbl would be exactly, the combined curve.

In general, then, the shape of the frequency of exceedance curve for spill volume at a single location is governed by two factors. The first is the range of possible volumes. Volume is determined from the diameter of the pipeline, topography, and location of valves. The second factor is the frequency with which each spill volume occurs. This is determined by the material and construction of the pipe, earthquake hazard, and number of elements which yield the same spill volume. In this application, the most important parameters were material and construction, and diameter of the pipe. In other applications, different parameters may be more important.

The single site dollar loss curve is shown in Figure 24. The minimum dollar loss at a single site is \$20,000, the maximum is \$840 million, and the expected value is \$3.6 million. This large range of dollar losses which can occur at a site is the result of the different types of environmental models and the variation in spill volumes. Figure 24 is plotted with a linear loss scale and its shape can be compared with the other loss curves presented in this section. This curve drops off very quickly, indicating that there is a very small range of values which are likely. The long tail of this curve also indicates that there is a large range of possible losses. The shape of this curve is considerably less smooth than that of the corresponding spill volume curve, Figure 23. This is due more to the different environmental models and failure probabilities of the pipes than the range of volumes possible.

The effect of the different probabilities of failure and environmental models can best be seen in Figure 25 which is the same single site dollar loss curve plotted with a logarithmic loss scale. While there is some overlap, sections of the curve have been labeled according to which groups of elements dominate the frequency of exceedance in that range of losses. In general, spills which occur away from surface water, including wetlands or floodplains, result in lower costs for remedial measures. Spills in wetlands or flood plains are the next most expensive to clean up, and spills in rivers or lakes are the most expensive. This is seen in Figure 25 as the general progression of environmental models.

There is some overlap of the dominant environmental model from \$9-60 million dollars due to the dependence on spill volume. As noted in the discussion of spill volumes, line 68 is most likely to have small spill volumes, while the Capline is likely to produce relatively large spill volumes. In the range from \$9-25 million, small spills in wetlands or floodplains occur approximately as often as large spills away from surface water. These occur with approximately the same frequency because the large number of Capline pipe elements away from surface water balances the fewer line 68 wetlands/floodplain elements, which are each more likely to fail.

This curve also indicates that dollar losses up to about \$9 million are most likely to occur on line 68 in elements which are away from surface water, including rivers, lakes, wetlands and floodplains. Based on change in exceedance frequency in this range, it can be determined that approximately 95 percent of all leaks occur on these elements. It is not surprising, then, that the expected value at a single site is only \$3.6 million.

The risk of losses for the region are expressed as probabilities of exceedance rather than frequencies because the probability of the event has been included in the simulation. In this example, 0.005 was used as the probability that this type of event will occur in the next 25 years.

The probability of exceedance for oil spills from the two major pipelines modeled is shown in Figure 26. Because there was at least one break in every simulation trial, the maximum exceedance probability is the same as the probability of the event, 0.005. The minimum total spill volume for the region is 108 thousand bbl, the maximum is 2.34 billion bbl, and the expected value is 410 thousand bbl, given the occurrence of the event. Not surprisingly, the expected value is approximately the average spill volume at a single site multiplied by the expected number of failures.

The shape of the total spill volume curve resembles that of the number of failures, rather than the spill volume at a single site. The variations in spill size from individual sites are smoothed out when many volumes are summed to obtain the total spill volume. In this application, then, the number of failures determines the shape of the total spill volume curve. In applications where the expected number of failures is closer to 1.0 than 100, the variation in spill volume at individual locations would be more significant.

*The risk of total dollar losses from a large NAEZ event is shown in Figure 27. The minimum total dollar loss is \$38 million, the maximum is \$2,360 billion, and the expected value is \$314 million. This implies that the expected conditional economic loss arising from oil contamination when  $m=8.6$  is  $\bar{L}(8.6) = 314$  million. This curve includes both the costs associated with remedial measures to restore the environment and the cost of repairing the pipelines. As was noted above, the cost of repairing the pipelines ranges from \$0.1-2.5 million, with an expected value of \$0.44 million. Since the direct damage losses are approximately two orders of magnitude less than the environmental losses, the total dollar loss curve is essentially the same as that for environmental losses alone. There are many possible combinations of environmental models, spill volumes and number of failures as well as several combinations which result in the same loss for almost any loss value. The result is that the total loss curve is very smooth and does not drop off as rapidly as the other curves. The analysis of this section is confined to the case of  $m=8.6$ . For the estimation of the expected annual economic loss  $L^*$ , the analysis must be performed for the scenario earthquakes with various values of  $m$ .*

## SECTION 7

### CONCLUSIONS AND RECOMMENDATIONS

The nation's urban lifeline systems are not only physically aging, but also becoming functionally obsolete. They require maintenance as a matter of routine, including regular and emergency repairs with an outlay of significant annual expenditures. In many cases, replacement and rehabilitation of some component facilities, if not the entire system, become more cost-effective than the continuation of the on-going maintenance procedure with the existing system even under the normal operating conditions.

Upgrading of seismic design guidelines and implementation of seismic retrofit ensure reduction of the annual expected economic loss and more balanced risk and reliability allocations among the component facilities, if it is done in accordance with such a conceptual and procedural framework as outlined here. One of the major incentives for having such a conceptual and procedural framework in place at this time is to assist the regulator and operator of lifelines in taking advantage of imminent replacement and rehabilitation opportunities to pursue correctly the seismic design guideline upgrading and retrofit implementation at minimal cost and system disruption. Another major incentive is that such a framework, once established, can always be referenced to check and verify the rationality of the complex process of developing seismic design and retrofit guidelines.

Further research is needed to examine the validity of these and other incentives for the voluntary adoption of both seismic standards for new facilities and retrofitting programs for existing facilities. Specifically, it is strongly urged to implement the guideline development as described here with an actual oil transmission or other lifeline systems.

**BLANK PAGE**

## SECTION 8

### REFERENCE

1. Algermissen, S.T. and Hopper, M.G. (1984). "Estimated Maximum Regional Seismic Intensities Associated With an Ensemble of Great Earthquakes that Might Occur Along the New Madrid Seismic Zone, East-Central United States," USGS Miscellaneous Field Studies Map MF- 1712, United States Geological Survey.
2. Ariman, T., Dobry, R., Grigoriu, M., Kozin, F., O'Rourke, M., O'Rourke, T. and Shinozuka, M. (1990). "Pilot Study on Seismic Vulnerability of Crude Oil Transmission Systems," NCEER Technical Report No. 90-0008, May 25.
3. Applied Technology Council (1988). "ATC-13, Earthquake Damage Evaluation Data for California."
4. Applied Technology Council (1991). "ATC-25, Seismic Vulnerability and Impact of Disruption of Lifelines in the Coterminous United States."
5. BSSC, 1988, NEHRP Recommended Provisions for the Development of Seismic Regulations for New Buildings, Federal Emergency Management Agency (Earthquake Hazard Reduction Series, Report 95, Washington, D.C.
6. Chang, S.E., Seligson, H.A. and Eguchi, R.T. (1995a). "Estimation of the Economic Impact of Multiple Lifeline Disruption: Memphis Light, Gas and Water Division Case Study," *NCEER Bulletin*.
7. Chang, S.E., Seligson, H.A. and Eguchi, R.T. (1995b). "Estimation of Economic Losses Caused by a Disruption of Lifeline Service," *lifeline Earthquake Engineering. Proceedings of the Fourth US Conference, San Francisco, CA, August 10- 12, ASCE Technical Council on Lifeline Earthquake Engineering, Monograph 6*, pp. 48-55.
8. Crespo, E., et al. (1987). "Ecuador Earthquakes of March 5, 1987," *EERI Newsletter*, Vol. 21, No. 7, July.
9. Dikkers, R.D., Chung, R.M., Mohraz, B., Lew, H.S., and Wright, R.N., Editors (1996). "Proceedings of a Workshop on Developing and Adopting Seismic Design and Construction Standards for Lifelines," NISTIR 5907.
10. EERI (1990). "Earthquake Spectra: Loma Prieta Earthquake Reconnaissance Report," Earthquake Engineering Research Institute, Supplement too Volume 6, May.
11. Ellingwood, B.R. (1980). "An investigation of the Miyagi-Ken-Oki, Japan Earthquake of June 12, 1978," National Bureau of Standards Special Publication 592.
12. Federal Emergency Management Agency (1995). *Plan for Developing and adopting Seismic Design Guidelines and Standards for Lifelines*, September.
13. Johnson, W.T. (1983). "Post-Earthquake Recovery in Natural Gas Systems-1971 San Fernando Earthquake," Earthquake Behavior and Safety of Oil and Gas Storage Facilities, Buried Pipelines and Equipment, pp. 386-388, *American Society of Mechanical Engineers*, New York.
14. Johnston, A.C. and S.J. Nava (1985), "Recurrence Rates and Probability Estimates for the

New Madrid Seismic Zone," *Journal of Geophysical Research*, Vol. 90, No. B7.

15. McCaffrey, M.A. and O'Rourke, T.D. (1983). "Buried Pipeline Response to Reverse Faulting During the 1971 San Fernando Earthquake," *Earthquake Behavior and Safety of Oil and Gas Storage Facilities Buried Pipelines and Equipment*, pp. 151-159, *American Society of Mechanical Engineers*, New York.
16. McNorgan, J.D. (1973). "Gas Line Response to Earthquakes," *Transportation Engineering Journal of ASCE*, Vol. 99, No. TE4, pp. 821-827.
17. Obermeier, S.F. (1985). "Nature of Liquefaction and Landslides in the New Madrid Earthquake Region," *Estimation of Earthquake Effects Associated with Large Earthquakes in the New Madrid Seismic Zone*, USGS Open File Report 985-457, United States Geological Survey.
18. O'Rourke, T.D. and Tawfiq, M.S. (1983). "Effects of Lateral Spreading on buried Pipelines During the 1971 San Fernando Earthquake," *Earthquake Behavior and Safety of Oil and Gas Storage Facilities Buried Pipelines and Equipment*, *American Society of Mechanical Engineers*, New York pp. 124-132.
19. Pelmulder, S.D., Eguchi, R.T. and Seligson, H.A. (1997). "Regional risk assessment of environmental contamination from oil pipelines," Technical Report of National Center for Earthquake Engineering Research (under preparation).
20. Peter I. Yanev, ed., (1978). "Miyagi-Ken-Oki Japan Earthquake June 12, 1978," EERI Earthquake Engineering Research Institute.
21. Phillips, S.H. and Virostek, J.K. (1990). "Natural Gas Disaster Planning and Recovery: The Loma Prieta Earthquake," Pacific Gas and Electric Company, San Francisco California.
22. Rose, A., Shinozuka, M. and Eguchi, R.T. "Engineering and Socioeconomic Analysis of a New Madrid Earthquake: Impacts of Electricity Lifeline Disruptions," *NCEER monograph*, forthcoming.
23. Rose, A., Benavides, J., Chang, S.F., Szczesmak, P. and Lim, D. (1995). "The Regional Economic Impact of an Earthquake: Direct and Indirect Effects of Electricity Lifeline Disruptions," *Journal of regional Science*.
24. Shinozuka, M., Ballantyne, D., Borchardt, R., Buckle I., O' Rourke, T. and Schiff A. (1995). "The Hanshin-Awaji Earthquake of January 17, 1995. Performance of Lifelines," Technical Report of National Center for Earthquake Engineering Research, Buffalo, New York.
25. Southern California Gas Company (1994). Letter to L. Thomas Tobin (California Seismic Safety Commission) from Don Dockray (Southern California Gas Company) dated 18 April.
26. Youd, T.L., Tinsley, J. C., Perkins, D.M., King, E.J. and Preston, R.F. (1978). "Liquefaction Potential Map of San Fernando Valley, California," *International Conference on Microzonation for Safer Construction-Research and Application*, 2d, San Francisco 1978, Proceedings, V.I., pp. 267-278.

**TABLE 1 Earthquakes Included In The Performance Summary  
In Reverse Chronological Order**

<b>Year</b>	<b>Location</b>	<b>Magnitude</b>
1995	Kobe, Japan	6.9
1994	Northridge, California	6.7
1992	Landers, California	7.4
1992	Big Bear, California	6.5
1989	Loma Prieta, California	7.1
1987	Whittier Narrows, California	5.9
1987	Ecuador	6.9
1986	San Salvador	5.4
1985	Mexico City	8.1 (& 7.9)
1985	Chile	7.8
1984	Morgan Hill, California	6.2
1983	Coalinga, California	6.7
1983	Borah Peak, Idaho	7.3
1983	Nihonkai-Chubu, Japan	7.7
1982	Miramichi, New Brunswick, Canada	5.7
1980	Kentucky	5.3
1980	Mammoth Lakes, California	6.1
1980	El Asnam, Algeria	7.2
1980	Southern Italy	7.0
1979	El Centro/Imperial Valley, California	6.6
1979	Coyote Lake, California	5.9
1979	Montenegro, Yugoslavia	6.6
1978/1979	Oaxaca and Guerrero, Mexico	7.8 (& 7.6)
1978	Miyagi-Ken-Oki./Sendai, Japan	7.4
1978	Santa Barbara, California	5.7
1978	Thessaloniki, Greece	6.5
1977	San Juan, Argentina	7.4
1977	Romania	7.2
1976	Tangshan, China	7.8
1976	Guatemala	7.5
1976	Mindanao, Philippines	8.0
1976	Fruili, Italy	6.5
1975	Haicheng, China	7.3
1975	Lice, Turkey	6.8
1975	Island of Hawaii	7.2
1974	Lima, Peru	7.6
1971	San Fernando Valley, California	6.6
1969	Santa Rosa, California	5.7
1964	Alaska	8.4
1964	Niigata, Japan	7.5
1952	Kern County, California	7.7
1940	Imperial Valley, California	7.1
1933	Long Beach, California	6.3
1923	Kanto, Japan	8.3
1906	San Francisco, California	8.3

**TABLE 2 Earthquakes Included In The Performance Summary  
In Order of Decreasing Magnitude**

Magnitude	Location	Year
8.4	Alaska	1964
8.3	San Francisco, California	1906
8.3	Kanto, Japan	1923
8.1 (& 7.9)	Mexico City	1985
8.0	Mindanao, Philippines	1976
7.8	Tangshan, China	1976
7.8 (& 7.6)	Oaxaca and Guerrero, Mexico	1978/1979
7.8	Chile	1985
7.7	Kern County, California	1952
7.7	Nihonkai-Chubu, Japan	1983
7.6	Lima, Peru	1974
7.5	Niigata, Japan	1964
7.5	Guatemala	1976
7.4	Landers, California	1992
7.4	San Juan, Argentina	1977
7.4	Miyagi-Ken-Oki/Sendai, Japan	1978
7.3	Haicheng, China	1975
7.3	Borah Peak, Idaho	1983
7.2	Island of Hawaii	1975
7.2	Romania	1977
7.2	El Asnam, Algeria	1980
7.1	Loma Prieta, California	1989
7.1	Imperial Valley, California	1940
7.0	Southern Italy	1980
6.9	Kobe, Japan	1995
6.9	Ecuador	1987
6.8	Lice, Turkey	1975
6.7	Northridge, California	1994
6.7	Coalinga, California	1983
6.6	San Fernando Valley, California	1971
6.6	El Centro/Imperial Valley, California	1979
6.6	Montenegro, Yugoslavia	1979
6.5	Big Bear, California	1992
6.5	Fruili, Italy	1976
6.5	Thessaloniki, Greece	1978
6.3	Long Beach, California	1933
6.2	Morgan Hill, California	1984
6.1	Mammoth Lakes, California	1980
5.9	Coyote Lake, California	1979
5.9	Whittier Narrows, California	1987
5.7	Santa Rosa, California	1969
5.7	Santa Barbara, California	1978
5.7	Miramichi, New Brunswick, Canada	1982
5.4	San Salvador	1986
5.3	Kentucky	1980

TABLE 3 Damage Categories of Selected Earthquakes

Damage Category	Year	Location	Magnitude
S	1995	Kobe, Japan	6.9
S	1994	Northridge, California	6.7
S	1989	Loma Prieta, California	7.1
S	1987	Ecuador	6.9
S	1978	Miyagi-Ken-Oki/Sendai, Japan	7.4
S	1971	San Fernando Valley, California	6.6
S	1964	Alaska	8.4
S	1964	Niigata, Japan	7.5
M/M	1992	Landers/Big Bear, California	7.4/6.5
M/M	1987	Whittier Narrows, California	5.9
M/M	1985	Chile	7.8
M/M	1984	Morgan Hill, California	6.2
M/M	1983	Coalinga, California	6.7
M/M	1983	Nihonkai-Chubu, Japan	7.7
M/M	1980	El Asnam, Algeria	7.2
M/M	1979	El Centro/Imperial Valley, California	6.6
M/M	1978	Santa Barbara, California	5.7
M/M	1976	Tangshan, China	7.8
M/M	1976	Guatemala	7.5
M/M	1975	Haicheng, China	7.3
M/M	1974	Lima, Peru	7.6
M/M	1969	Santa Rosa, California	5.7
M/M	1952	Kern County, California	7.7
M/M	1933	Long Beach, California	6.3
M/M	1923	Kanto, Japan	8.3
M/M	1906	San Francisco, California	8.3
None	1986	San Salvador	5.4
None	1985	Mexico City	8.1 (& 7.9)
None	1983	Borah Peak, Idaho	7.3
None	1982	Miramichi, New Brunswick, Canada	5.7
None	1980	Kentucky	5.3
None	1980	Mammoth Lakes, California	6.1
None	1980	Southern Italy	7.0
None	1979	Coyote Lake, California	5.9
None	1979	Montenegro, Yugoslavia	6.6
None	1978/1979	Oaxaca and Guerrero, Mexico	7.8 (& 7.6)
None	1978	Thessaloniki, Greece	6.5
None	1977	San Juan, Argentina	7.4
None	1977	Romania	7.2
None	1976	Mindanao, Philippines	8.0
None	1976	Fruili, Italy	6.5
None	1975	Lice, Turkey	6.8
None	1975	Island of Hawaii	7.2
None	1940	Imperial Valley, California	7.1

\*S - Significant Damage Noted, M/M - Moderate to Minor Damage Noted, None = No Damage Reported

**Table 4 Damage Probability Matrix Based on Expert Opinion for  
Low-Rise Reinforced Concrete Shear-Wall Buildings  
(with Moment-Resisting Frame)**

Central Damage Factor	Modified Mercalli Intensity						
	VI	VII	VIII	IX	X	XI	XII
0.00	18.1	***	***	***	***	***	***
0.50	69.8	17.8	0.6	***	***	***	***
5.00	12.1	82.2	97.7	71.8	14.6	0.3	***
15.00	***	***	1.7	28.2	83.2	68.8	29.4
45.00	***	***	***	***	2.2	30.9	70.4
80.00	***	***	***	***	***	***	0.2
100.00	***	***	***	***	***	***	***

\*\*\* Very small probability.

**TABLE 5 Pipeline Exposure in a Magnitude 8.6 Earthquake in the NMSZ  
(Thousands of Feet)**

HAZARD	LINE 68	CAPLINE
MMI VII Only	1430	54
MMI VIII Only	885	1336
MMI IX Only	493	103
MMI X Only	0	40
Liquefaction Potential & MMI IX	166	1178
Liquefaction Potential & MMI X-XI	0	0
Total Footage	2974	2711

**TABLE 6 Remediation Cost Schedule for all Models**

ITEM	LOW CASE	HIGH CASE
Soil Remediation	\$100 /cubic yd.	\$150 /cubic yd.
Small Well System	\$38,000	\$47,000
Larger Well System	\$380,000	\$470,000
Light Oil Disposal	\$0.85 / gal.	\$1.50 /gal.
Heavy Oil Disposal	\$3.50 /gal.	\$6.00 /gal.

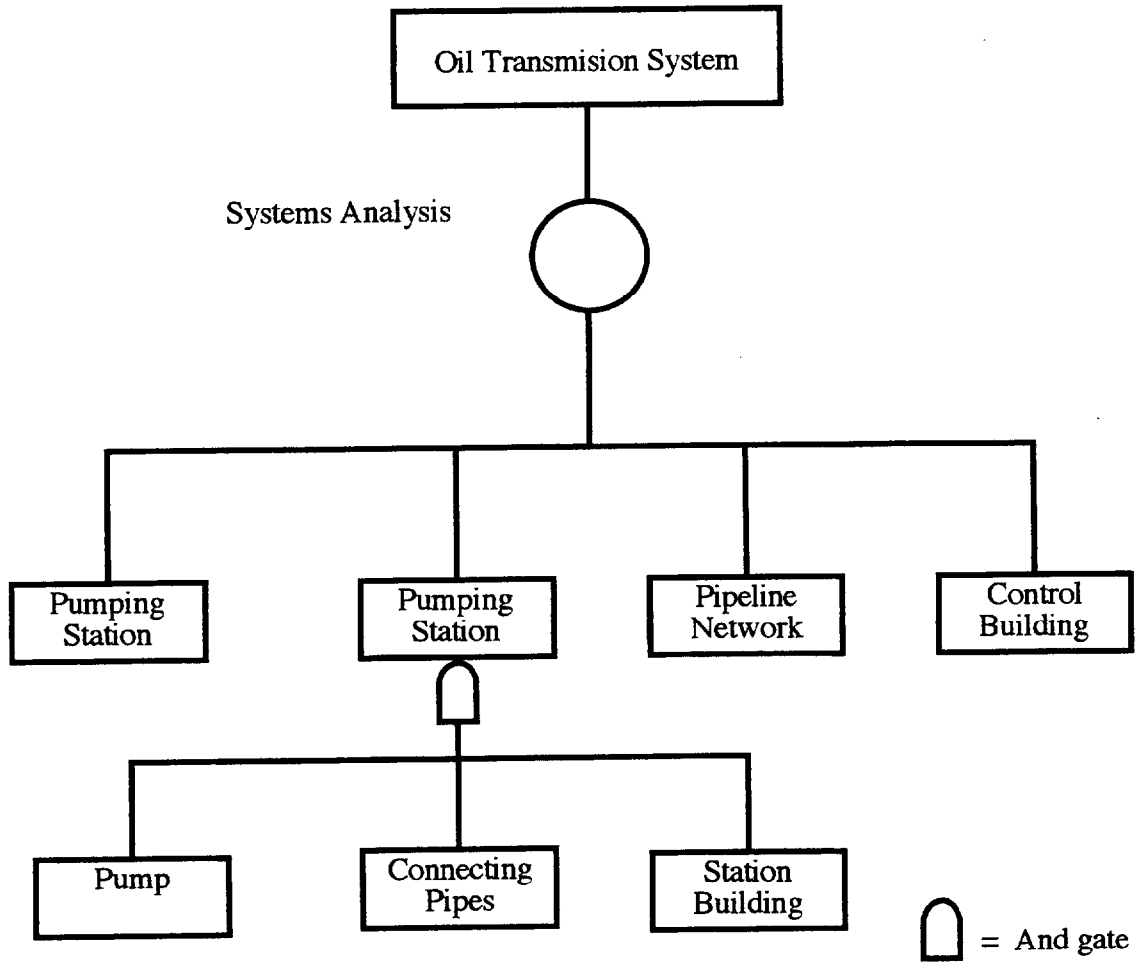


Figure 1. Schematic fault tree-like depiction of an oil transmission system

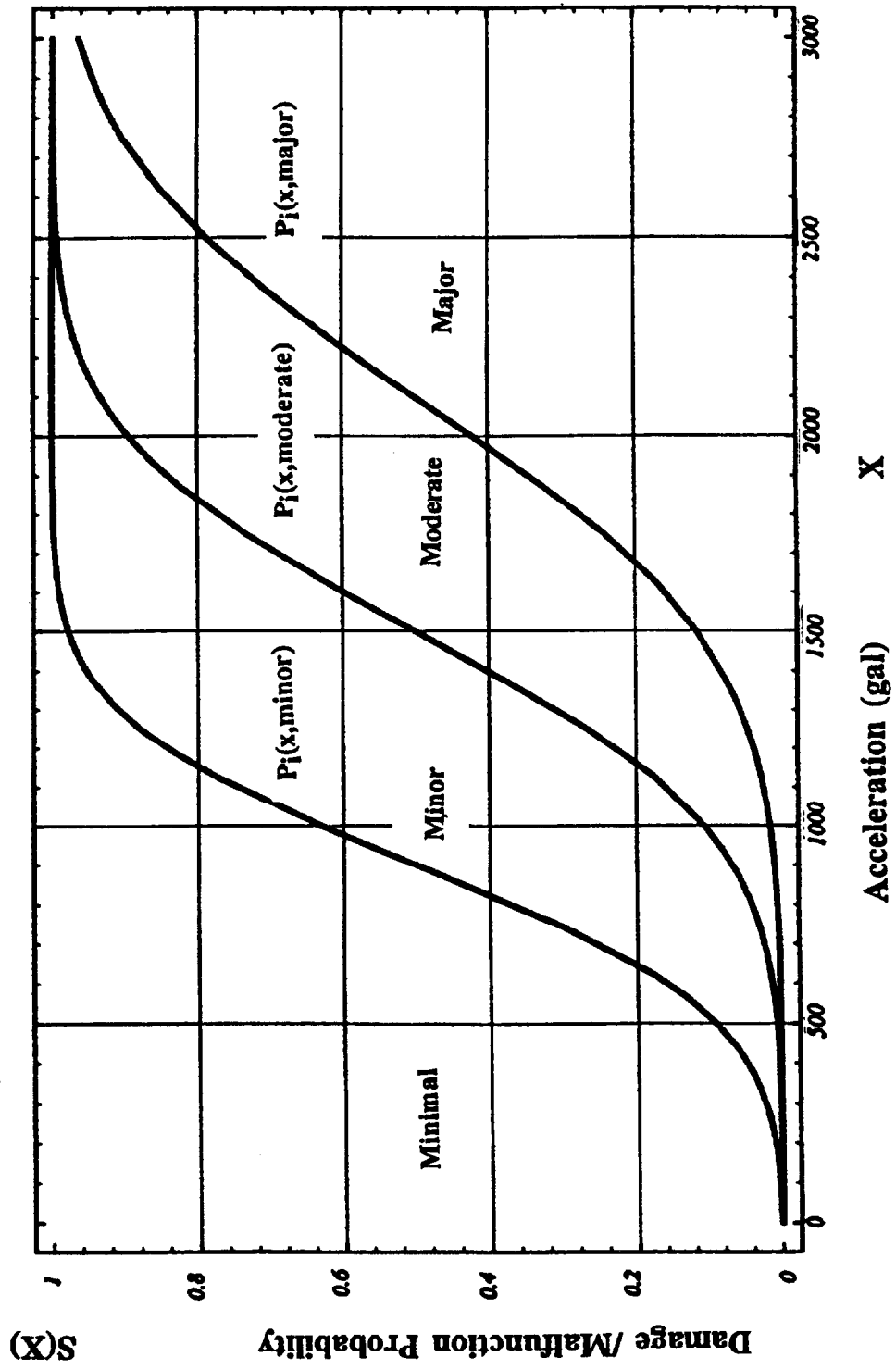
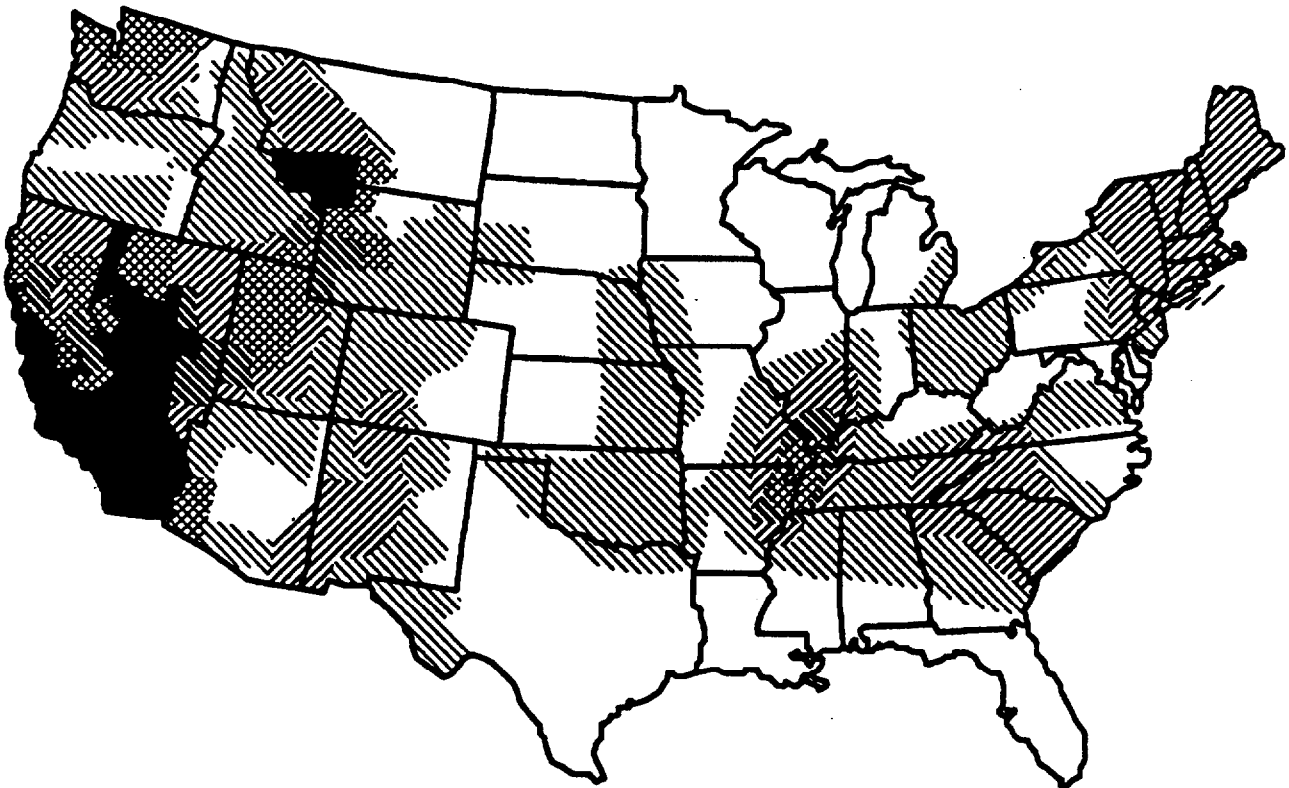


Figure 2. A family of component fragility curves



**Legend**

Map Area	Coeff. $A_s$
7	0.40
6	0.30
5	0.20
4	0.15
3	0.10
2	0.05
1	0.05

Figure 3. NEHRP Seismic Map Areas (BSSC, 1988)

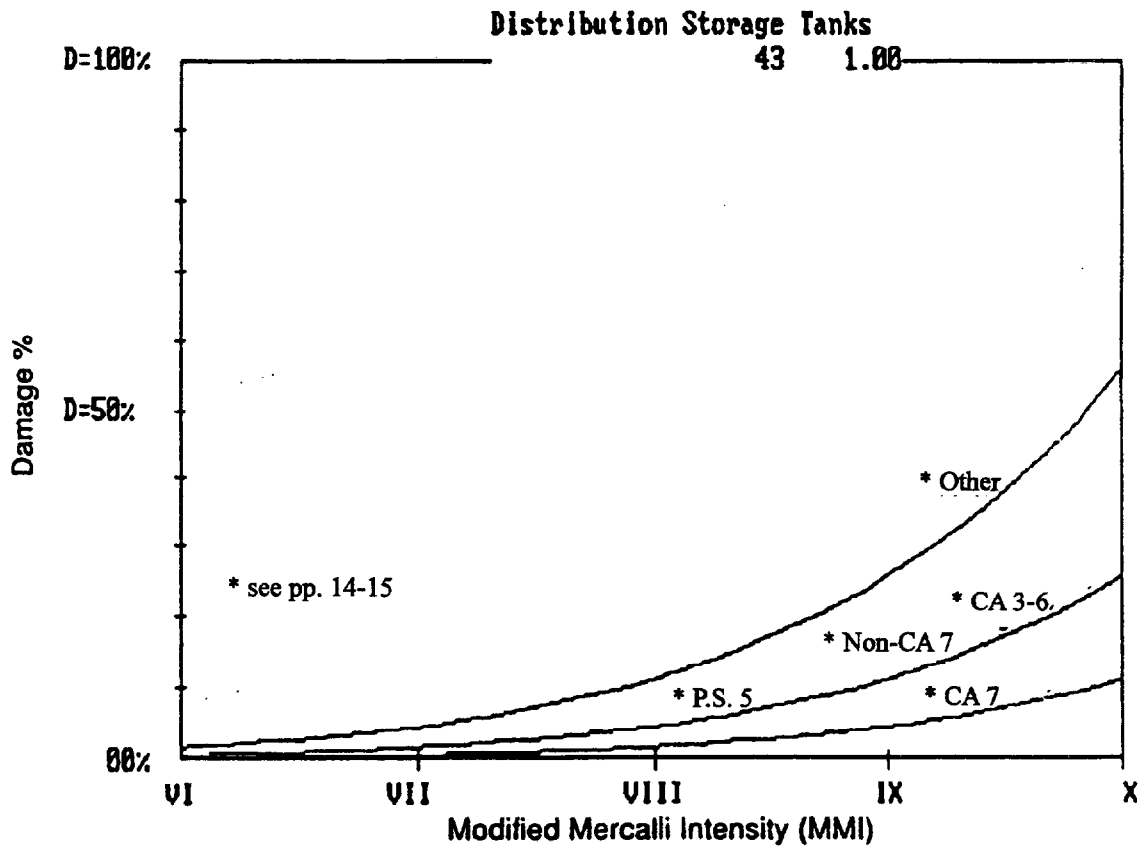


**Figure 4. Damage percent by intensity for petroleum fuels distribution storage tanks.**

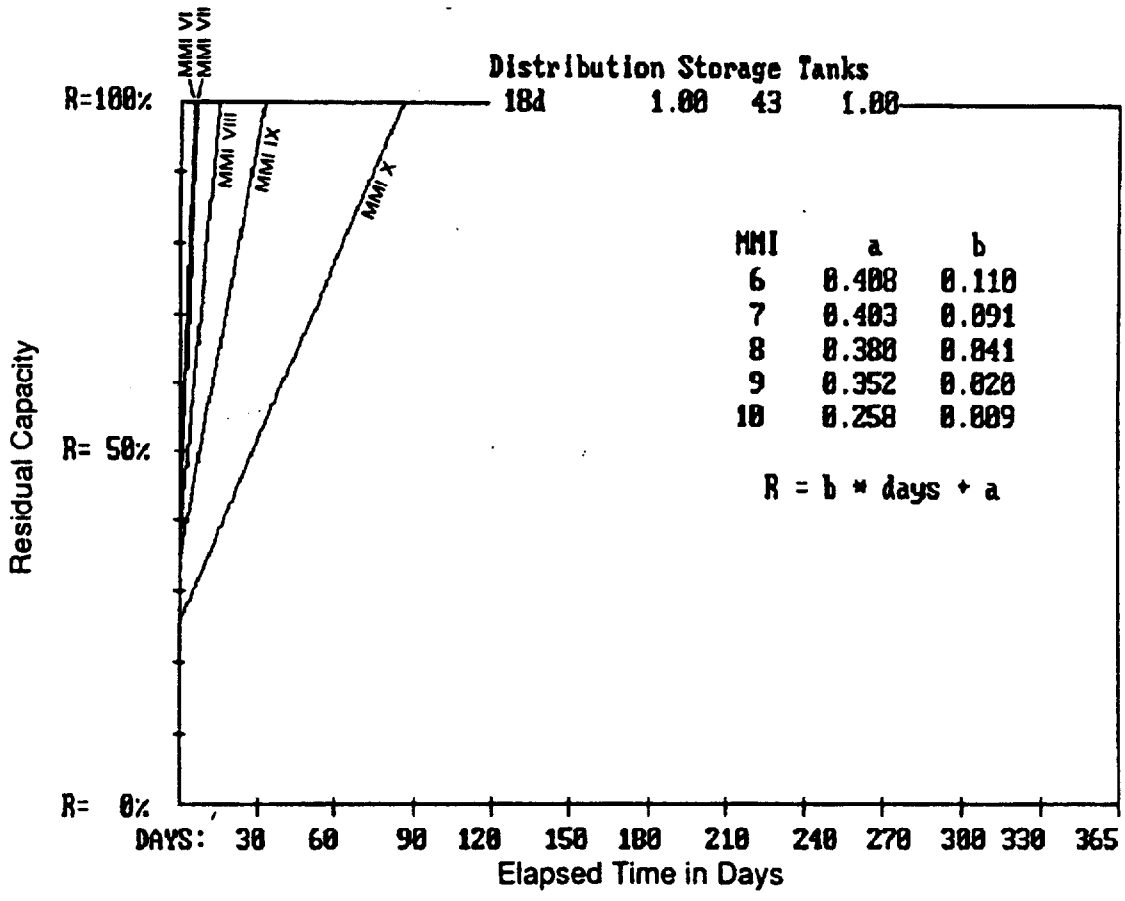


Figure 5. Residual capacity for petroleum fuels distribution storage tanks (NEHRP California 7)

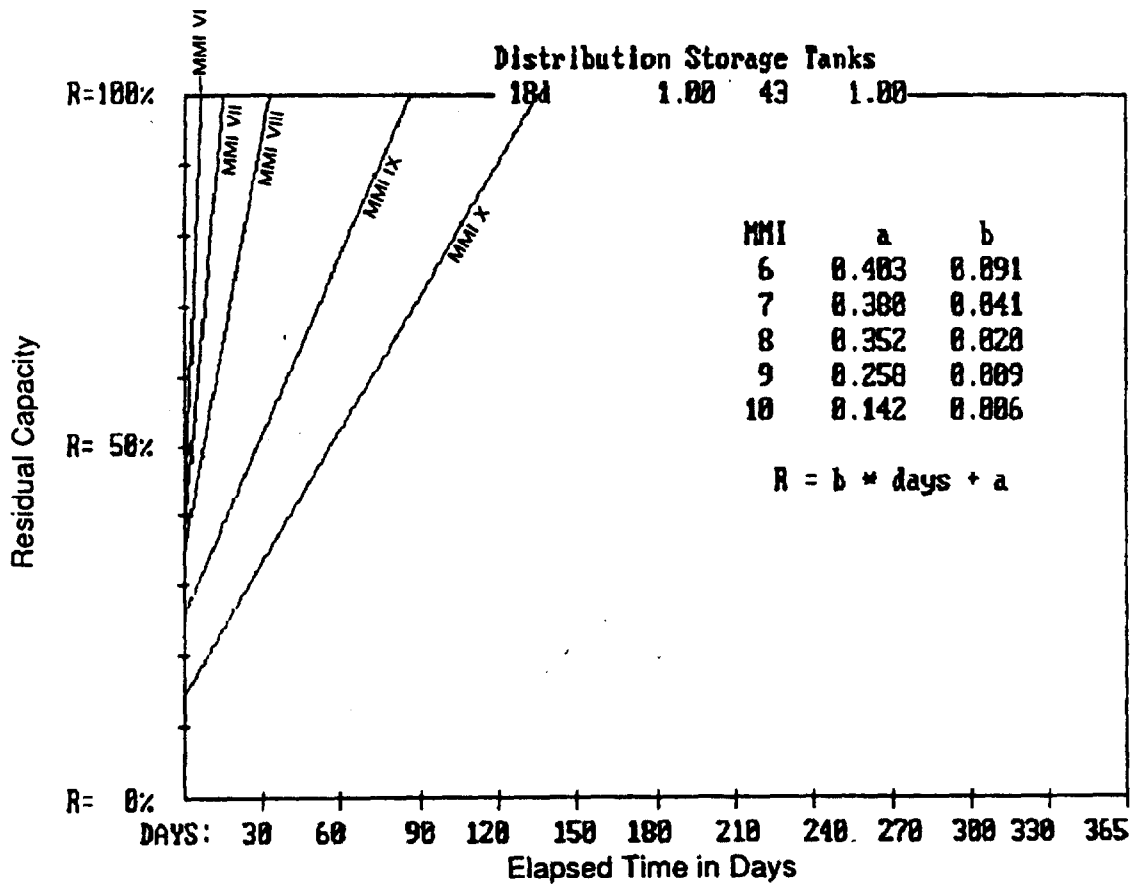


Figure 6. Residual capacity for petroleum distribution storage tanks (NEHRP Map Area : California 3-6, Non-California 7, and Puget Sound 5).

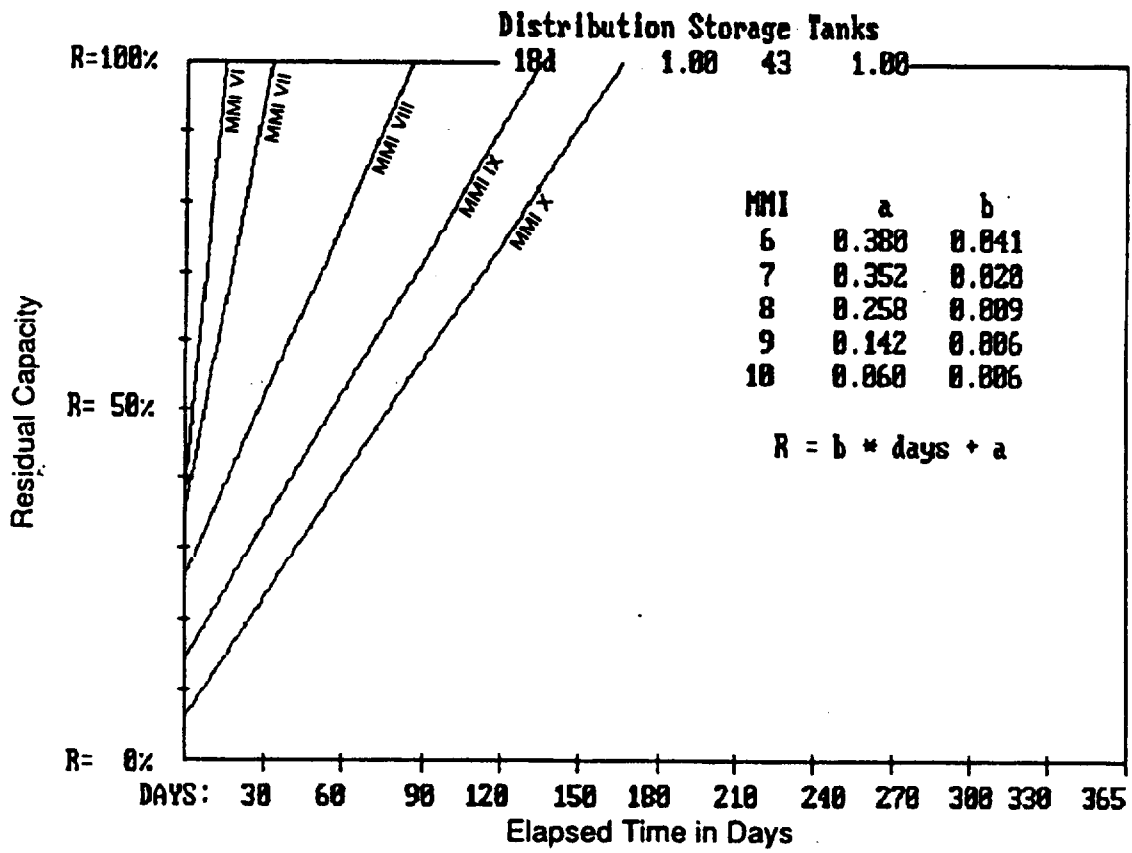
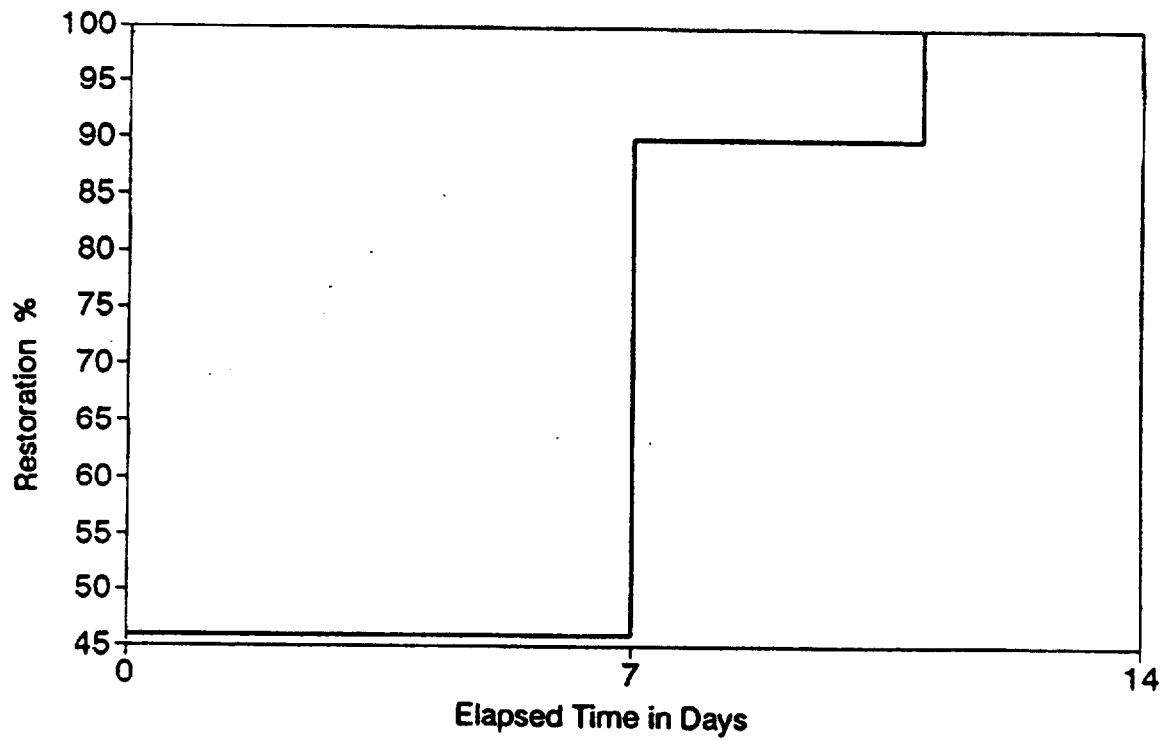


Figure 7. Residual capacity for petroleum fuels distribution storage tanks (All other areas).



**Figure 8. Residual capacity of crude oil delivery from Texas and Louisiana to Chicago following New Madrid event (M=8.0)**

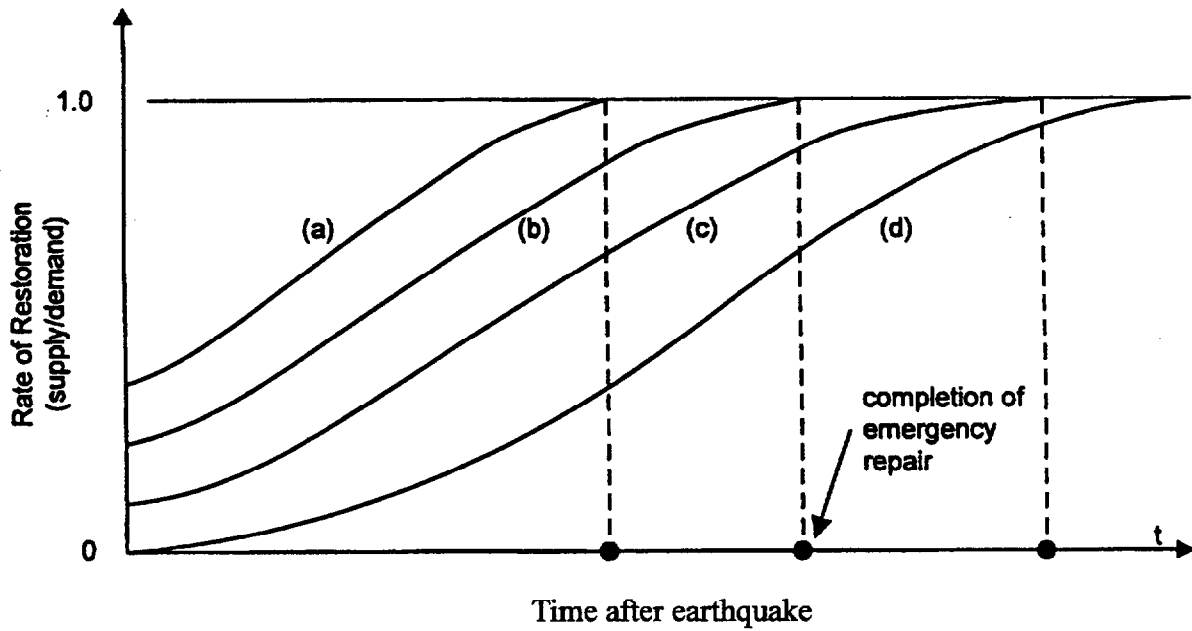


Figure 9a. Simplified restoration curves

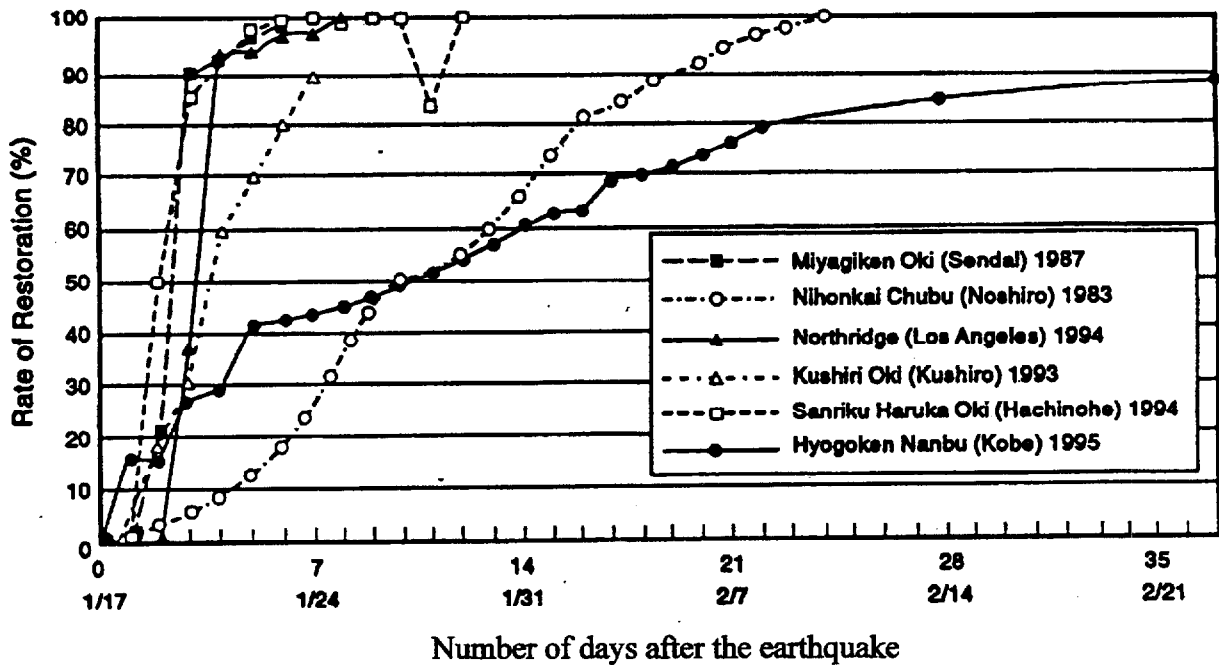


Figure 9b. Actual restoration curves for different water delivery systems

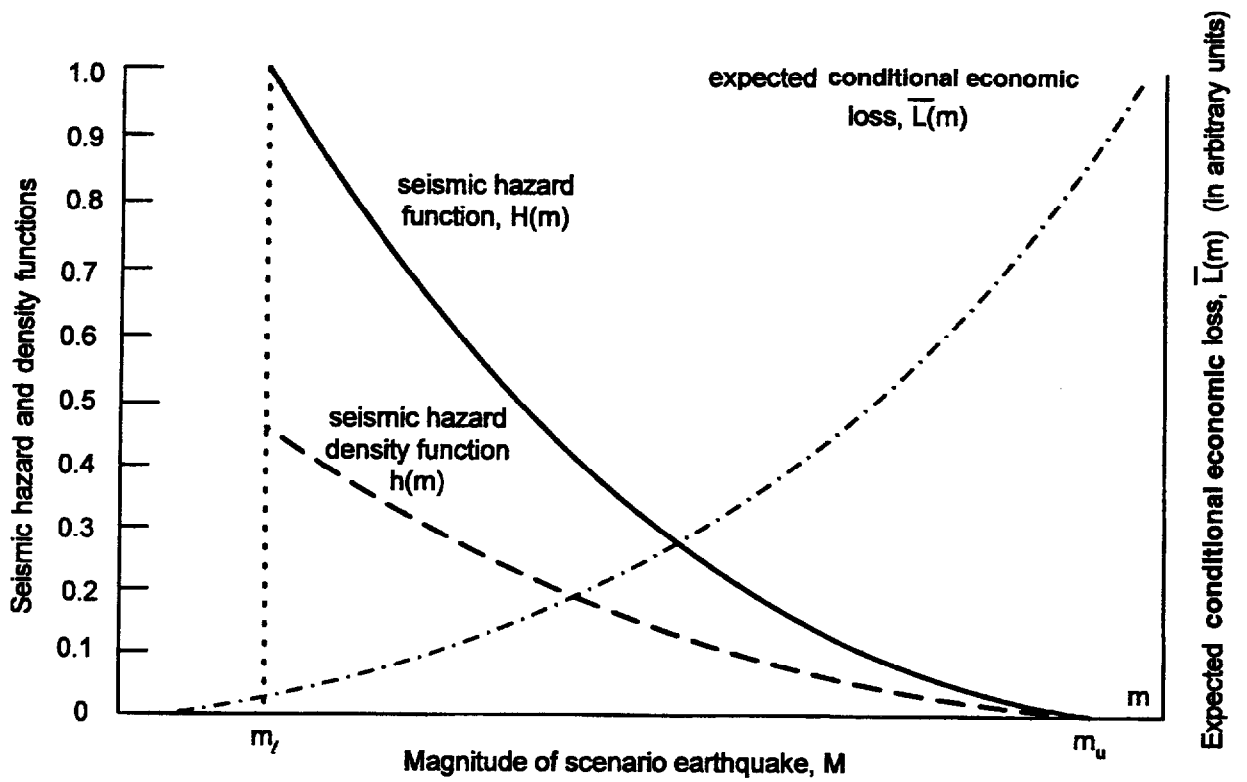


Figure 10. Seismic hazard function,  $H(m)$ , and seismic hazard density,  $h(m) = -dH(m)/dm$ , and expected conditional economic loss,  $\bar{L}(m)$

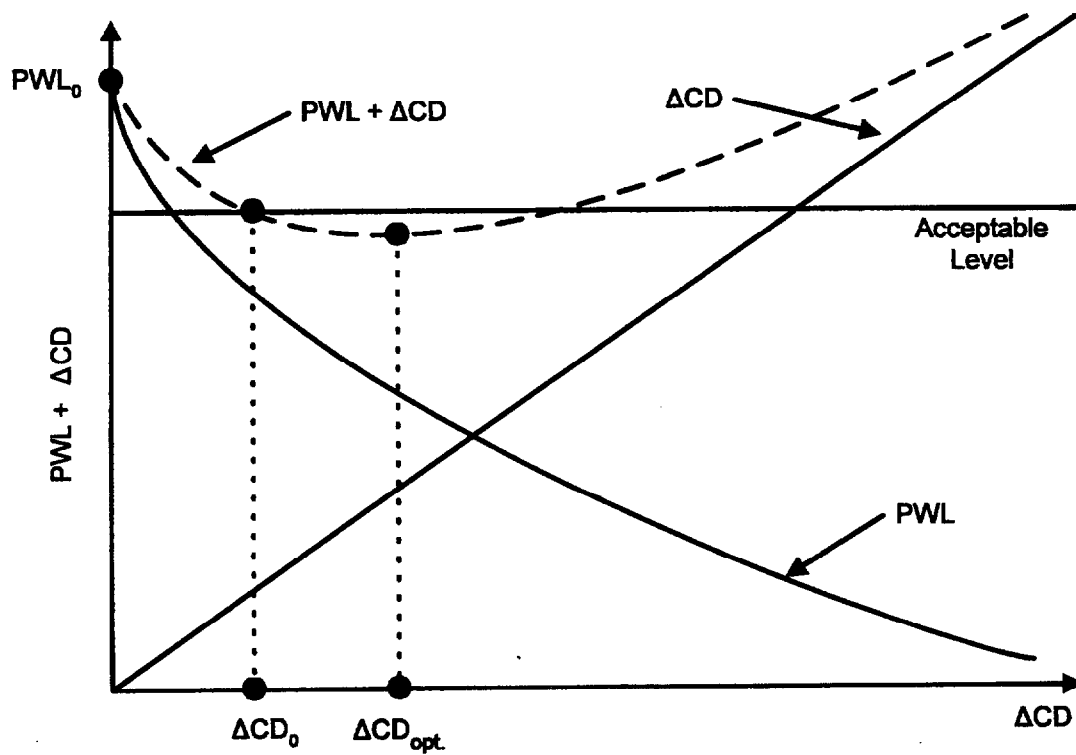


Figure 11. Optimal level of design guideline upgrading

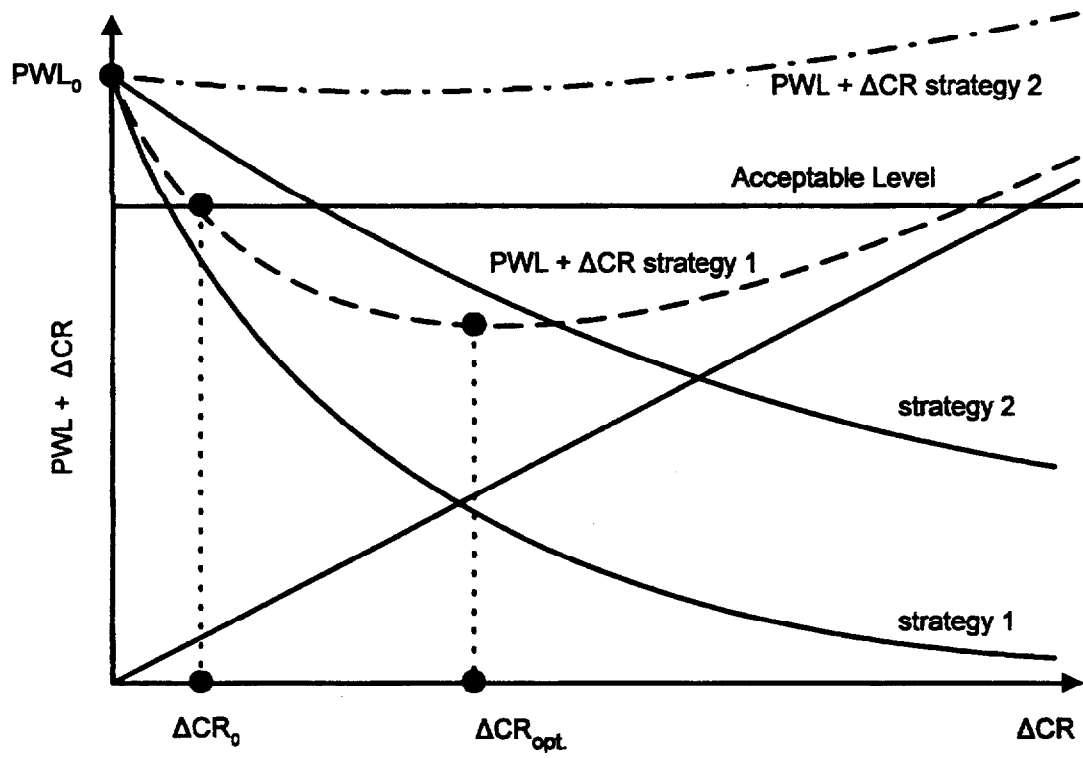


Figure 12. Optimal strategy and level of retrofit

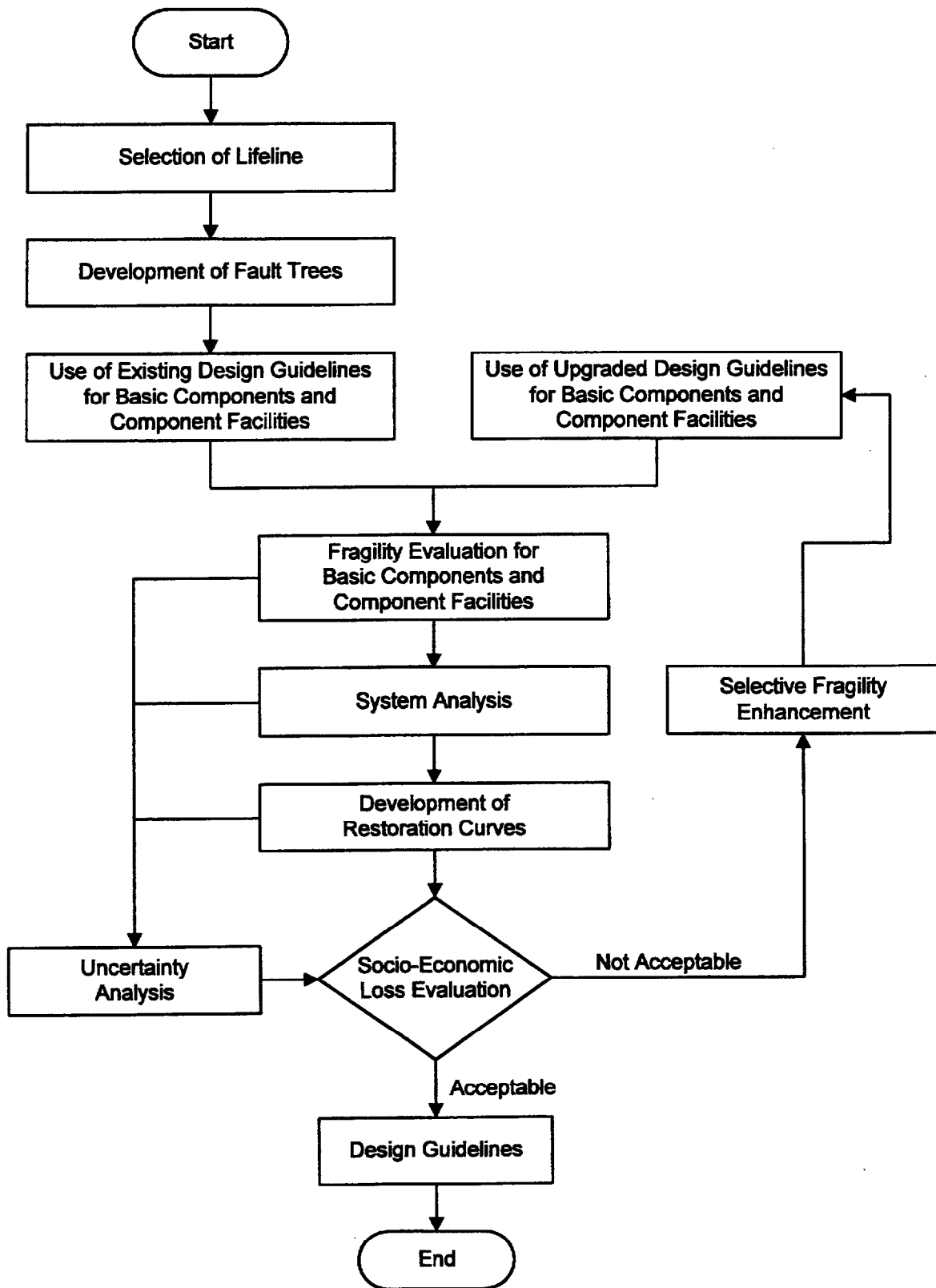


Figure 13. Flow chart for development of design guidelines

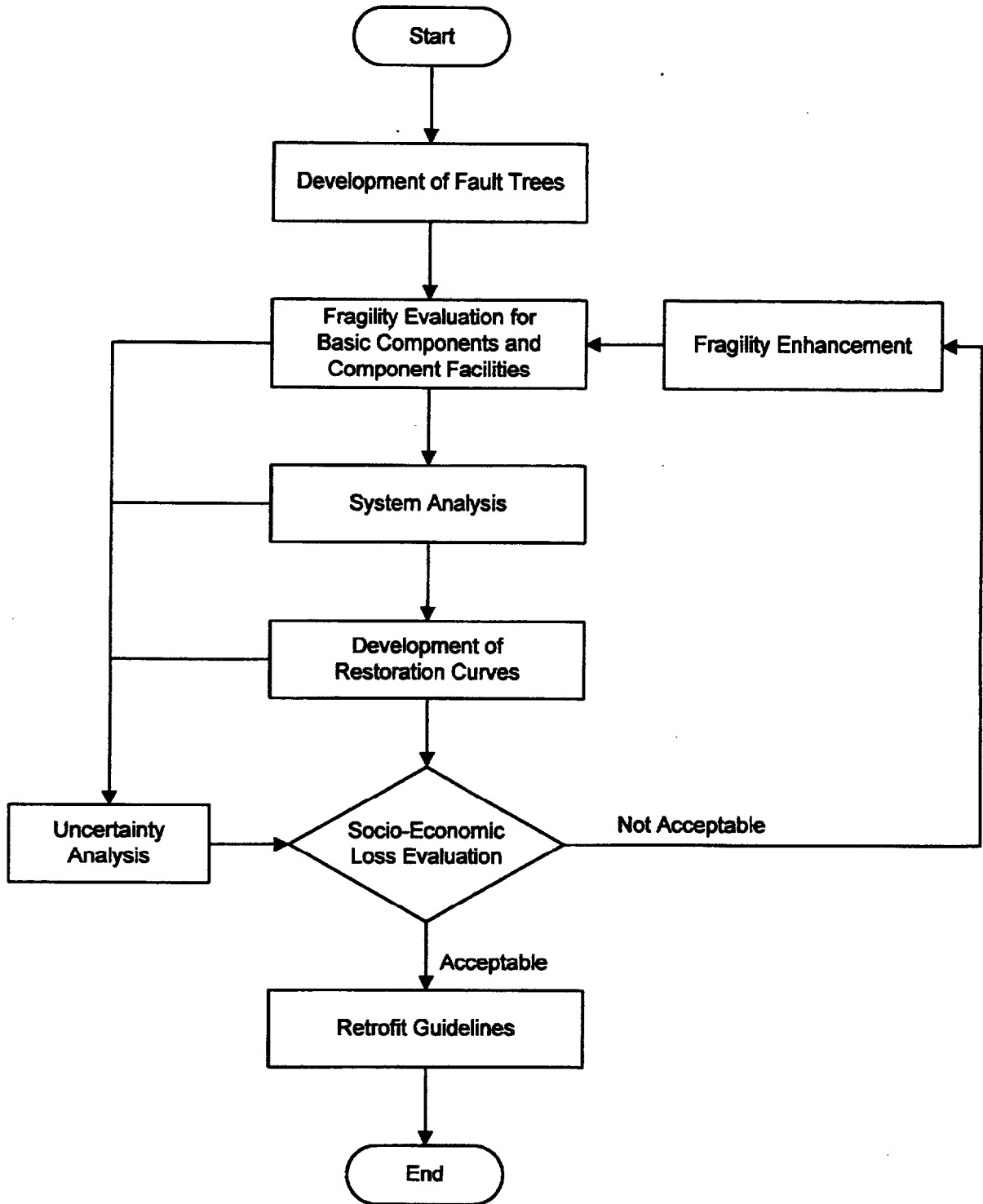


Figure 14. Flow chart for execution of retrofit procedures

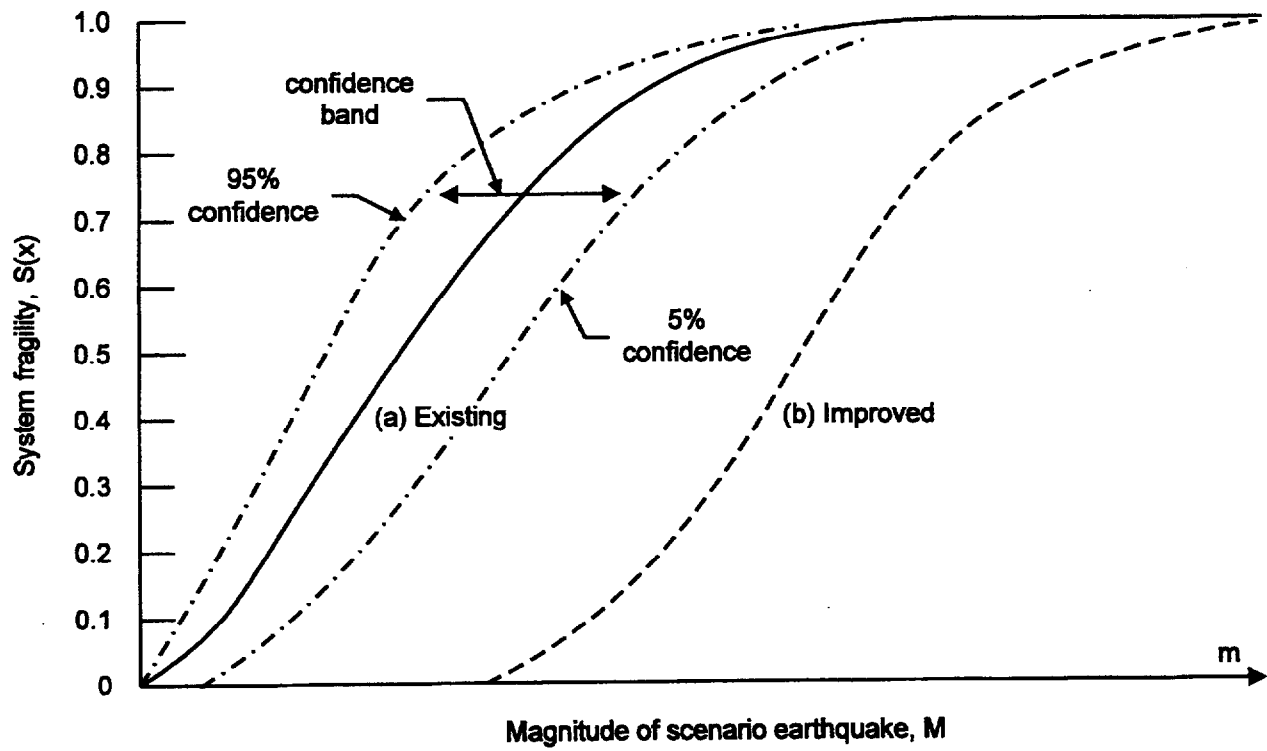


Figure 15. Component fragility curves

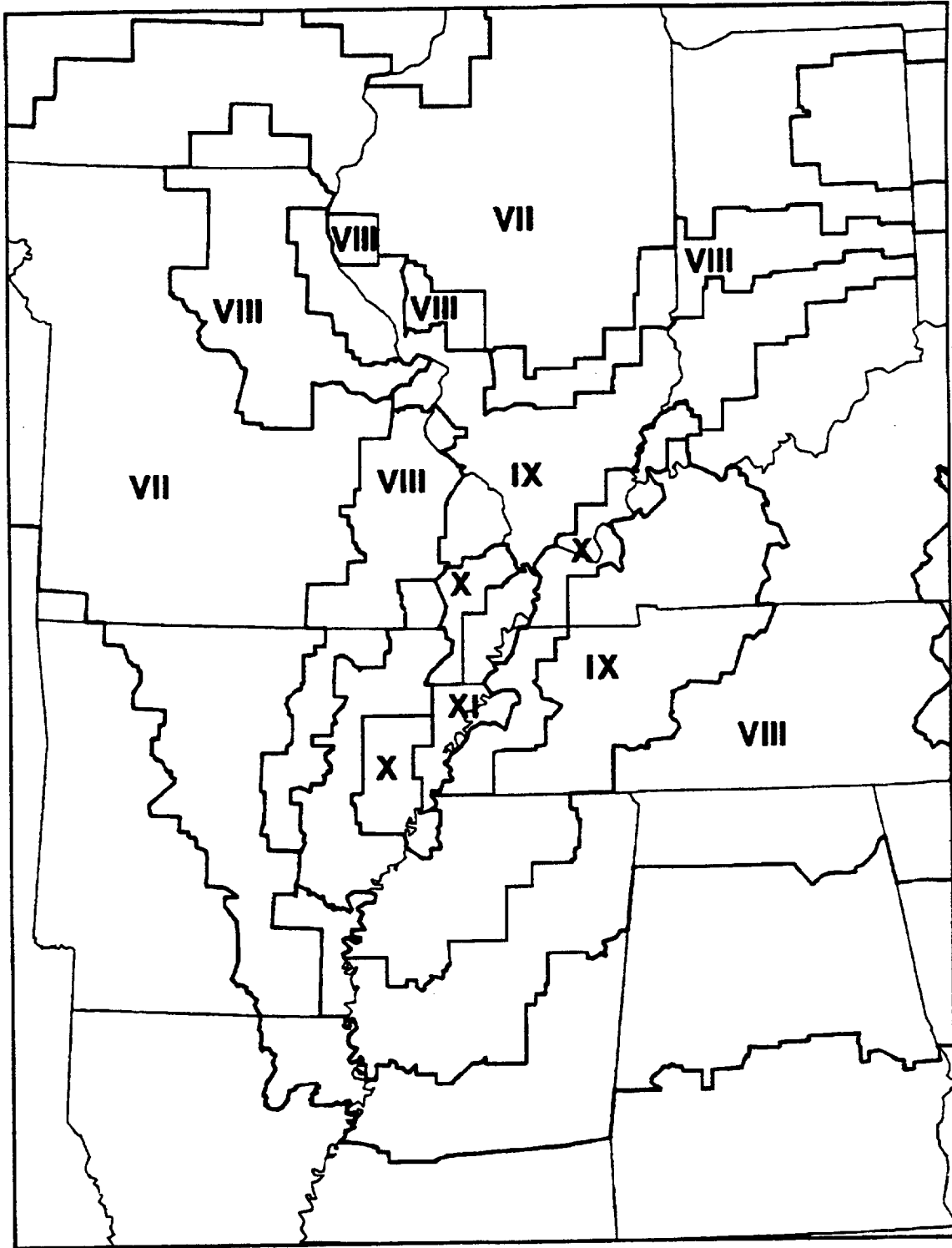


Figure 16: Modified Mercalli Intensity for a Magnitude 8.6 Event Anywhere Along the New Madrid Seismic Zone. (Digitized from Algermissen and Hopper, 1984)

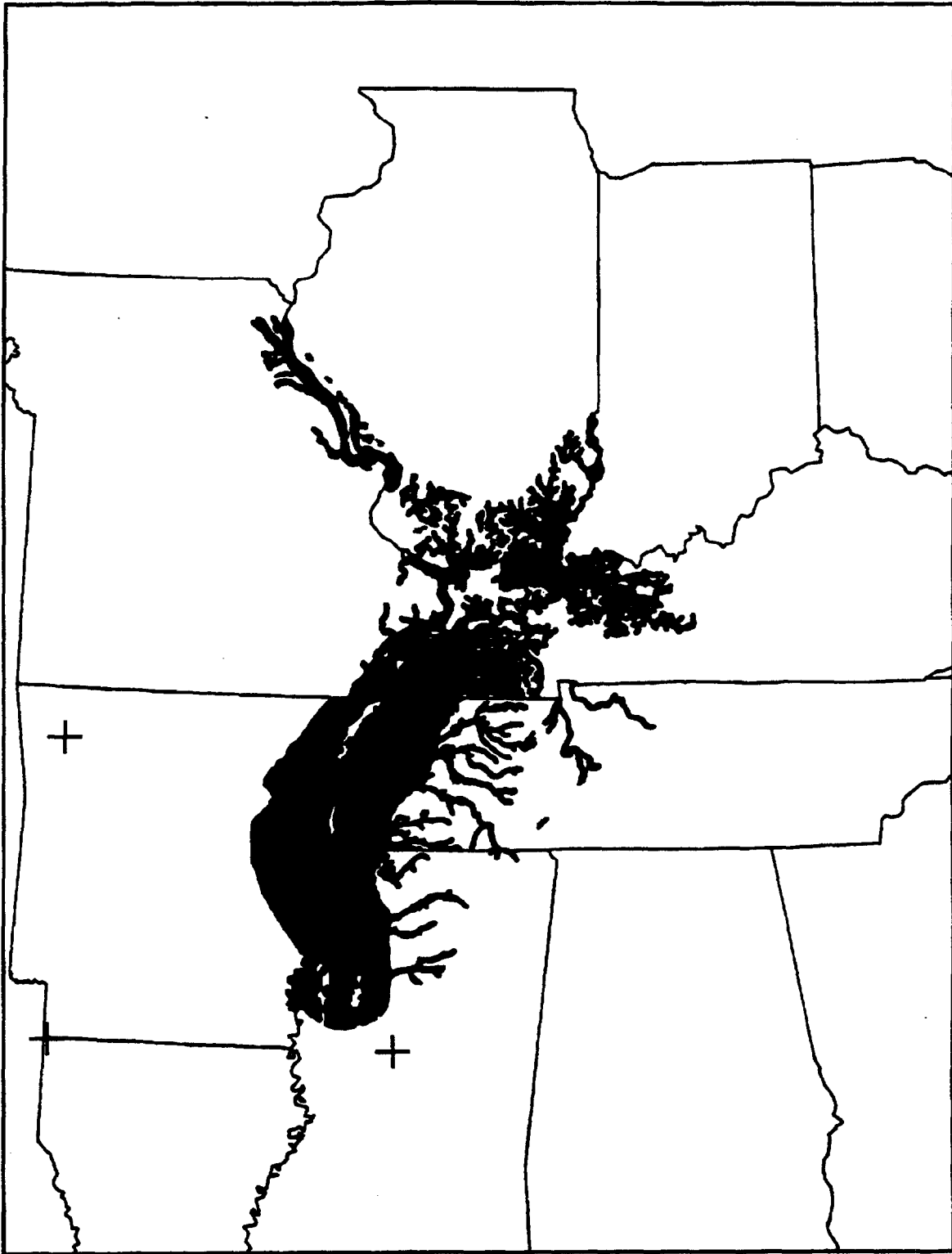


Figure 17: Areas of Moderate to High Liquefaction Potential in a Major New Madrid Seismic Event. (Digitized from Obermeier, 1984)

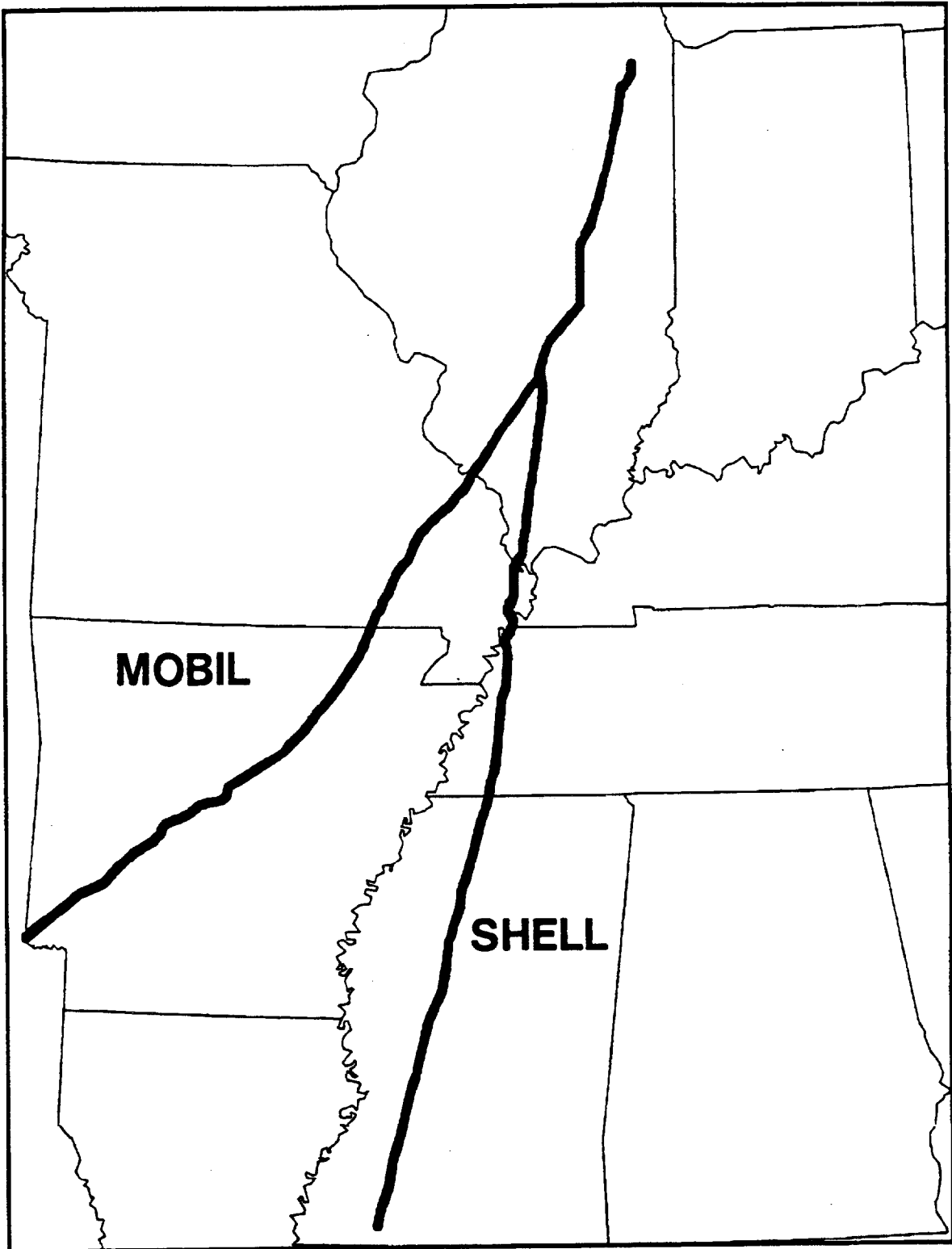


Figure 18: Pipelines Studied

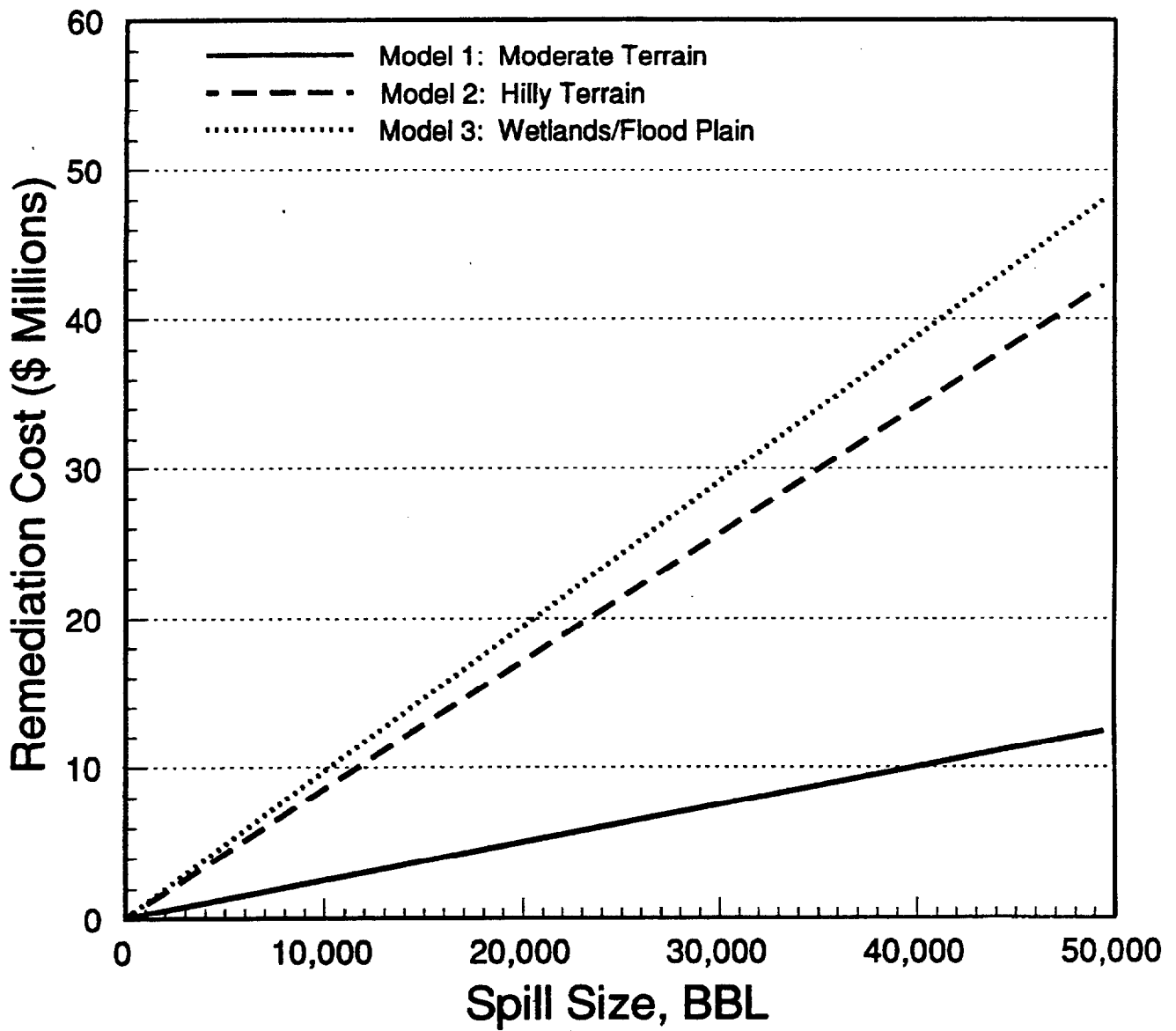
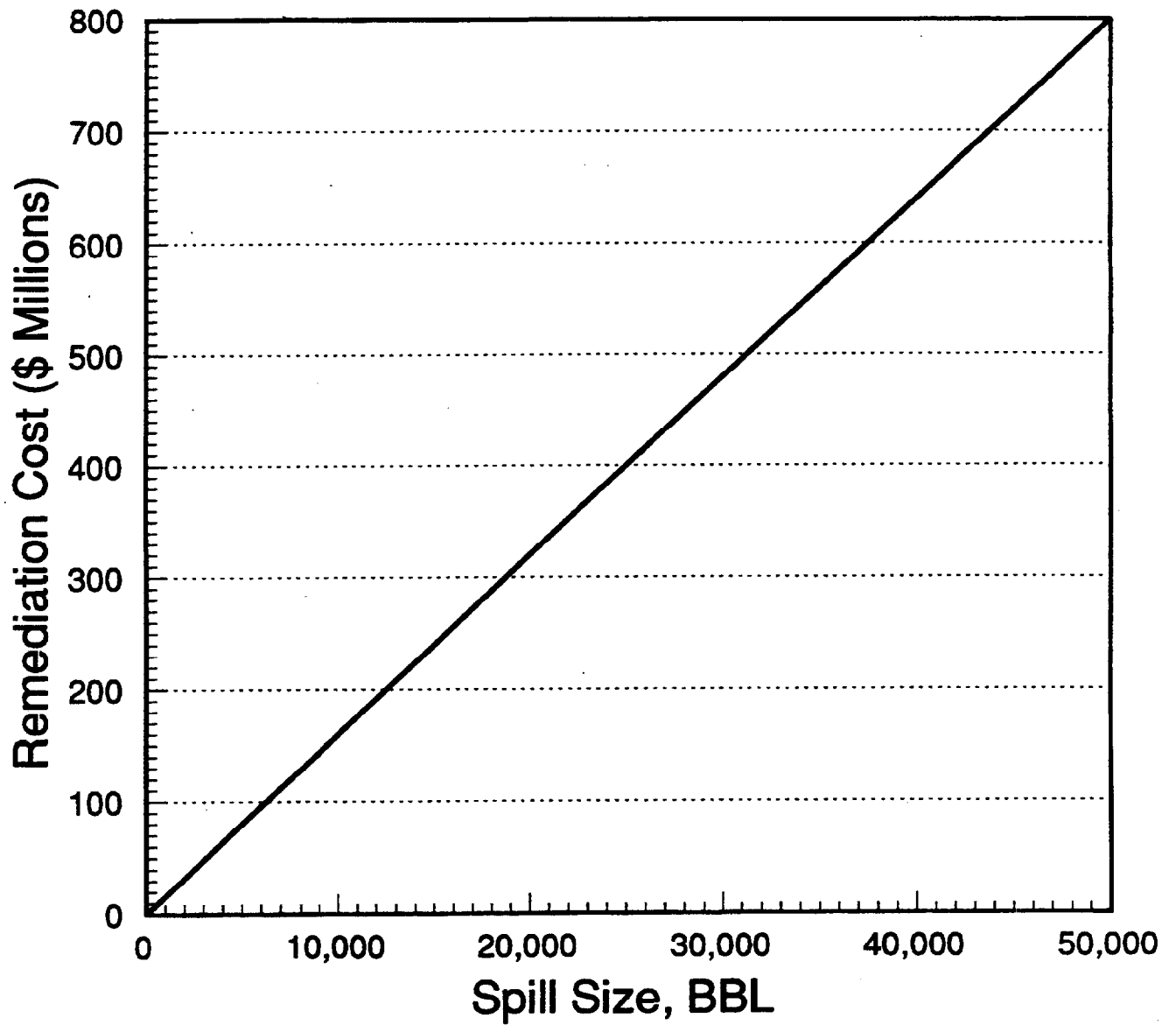


Figure 19: Remediation Cost vs. Spill Size for Example, Models 1-3



**Figure 20: Remediation Cost vs. Spill Size for Example, Models 5:  
Near Rivers with Shallow Cover**



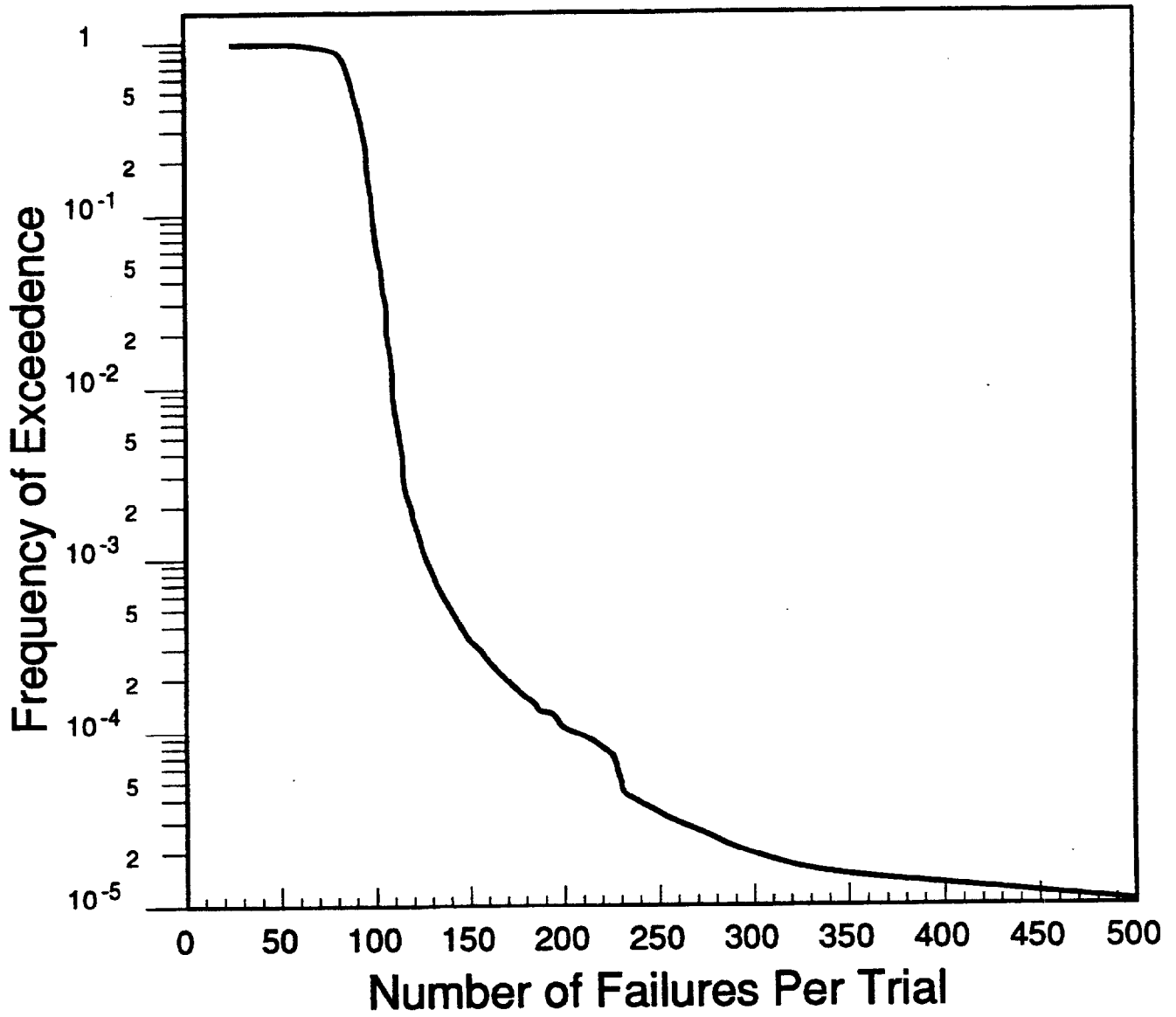
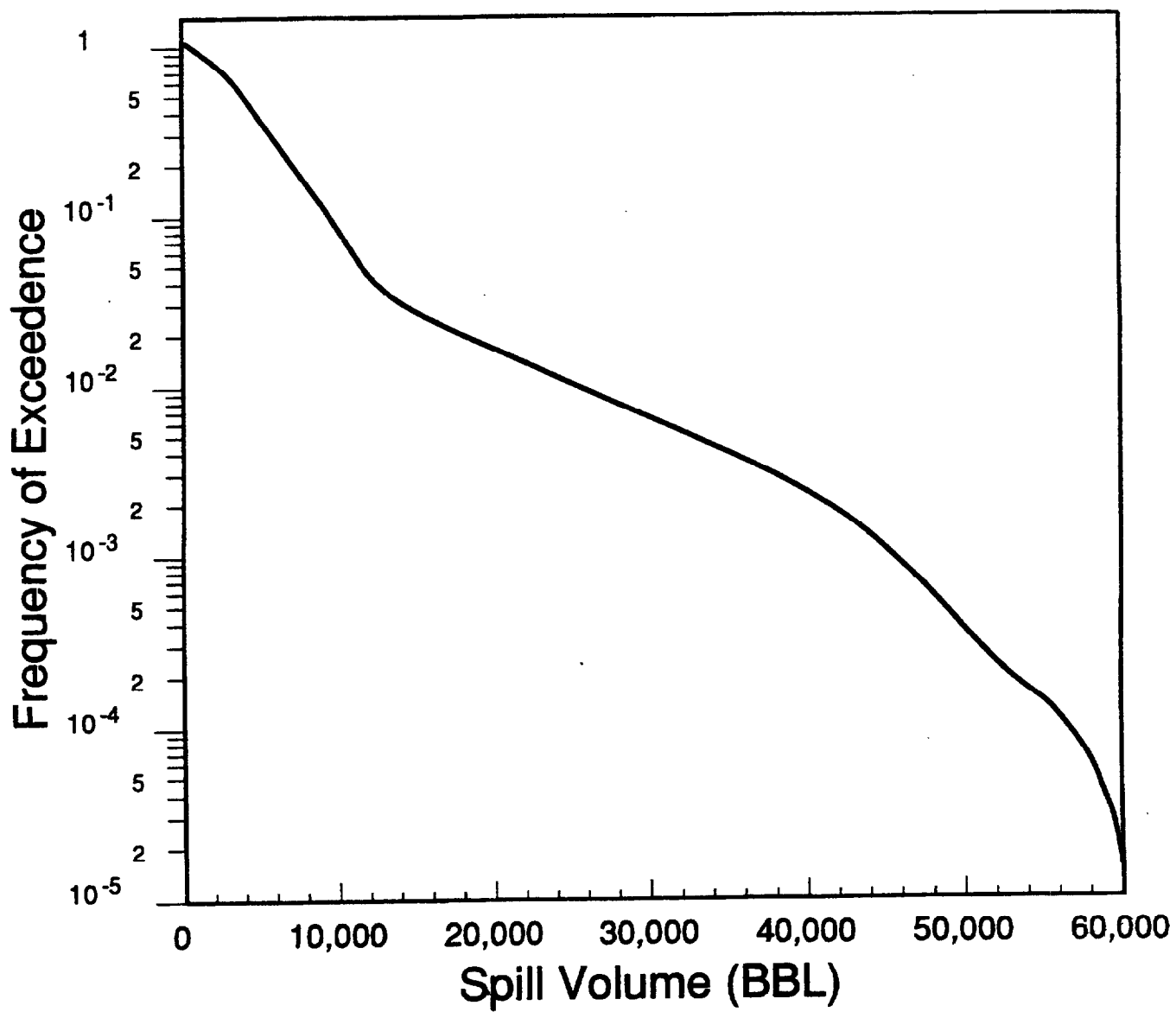


Figure 22: Direct Damage to Pipelines Given a Large NMSZ Event



**Figure 23 : Spill Volume at a Single Site,  
Given the Occurrence of a Large NMSZ Event**

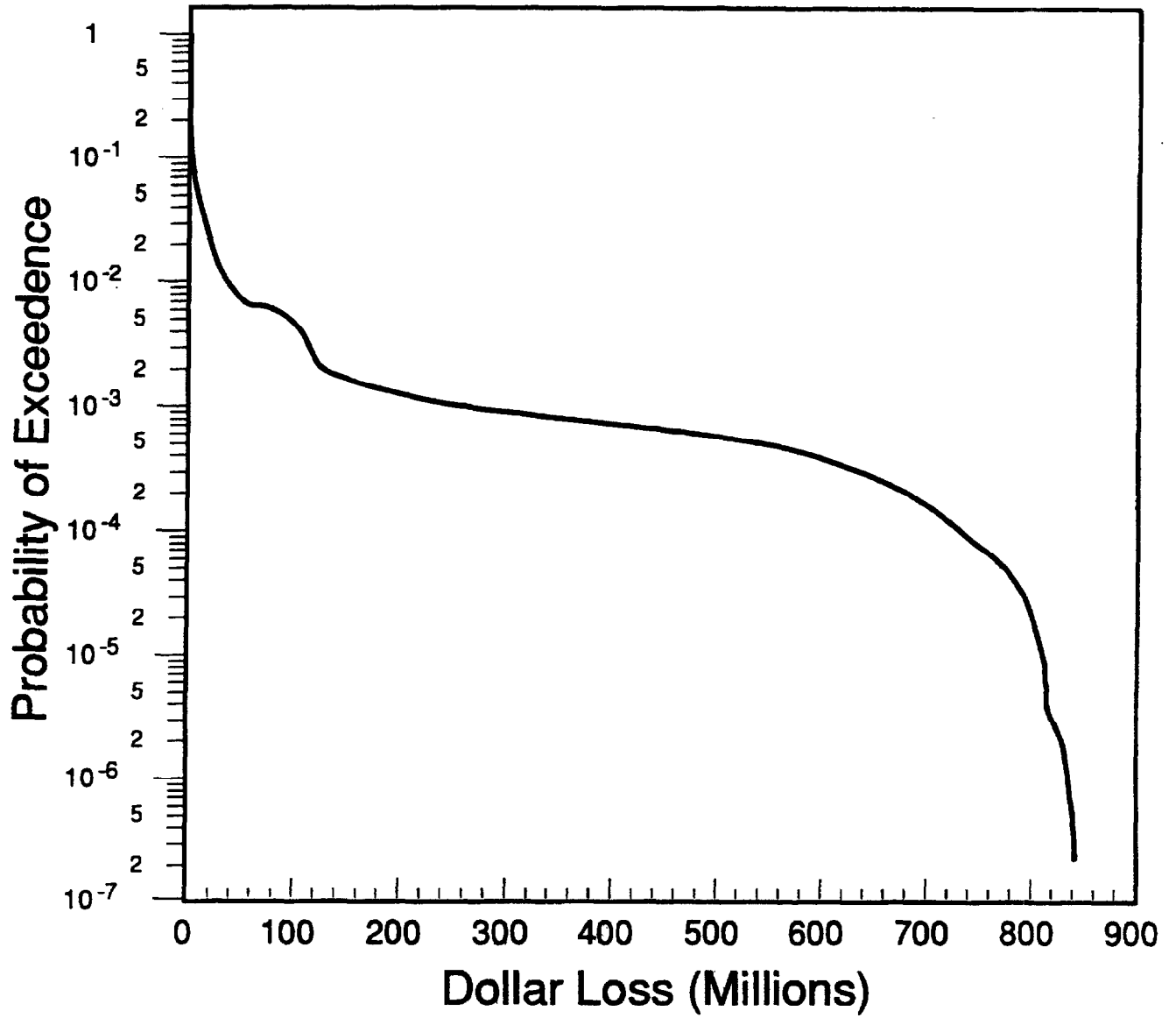


Figure 24: Dollar Loss at a Single Site, Given a Large NMSZ Event

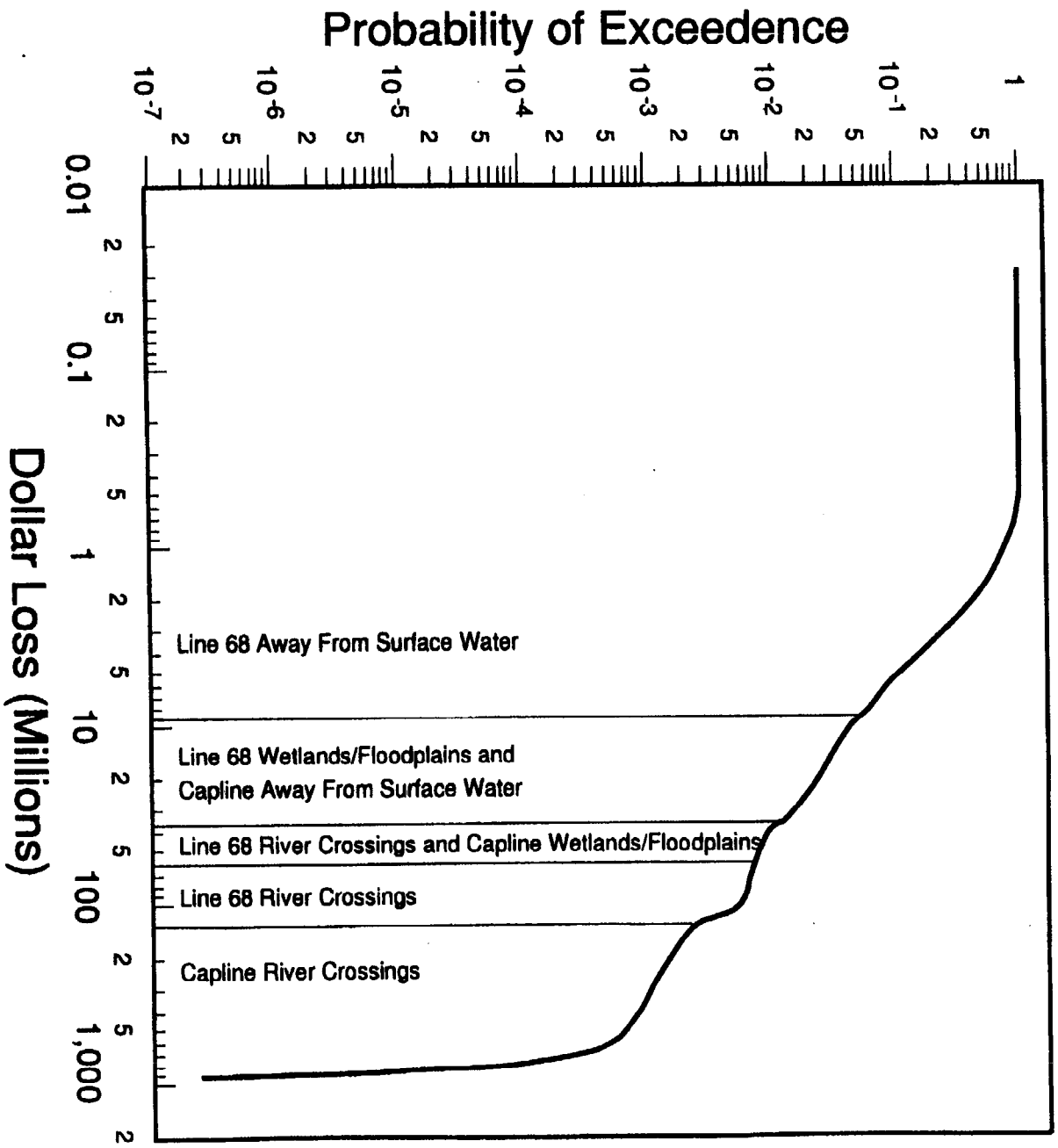


Figure 25: Dominant Environmental Models in Dollar Loss at a Single Site

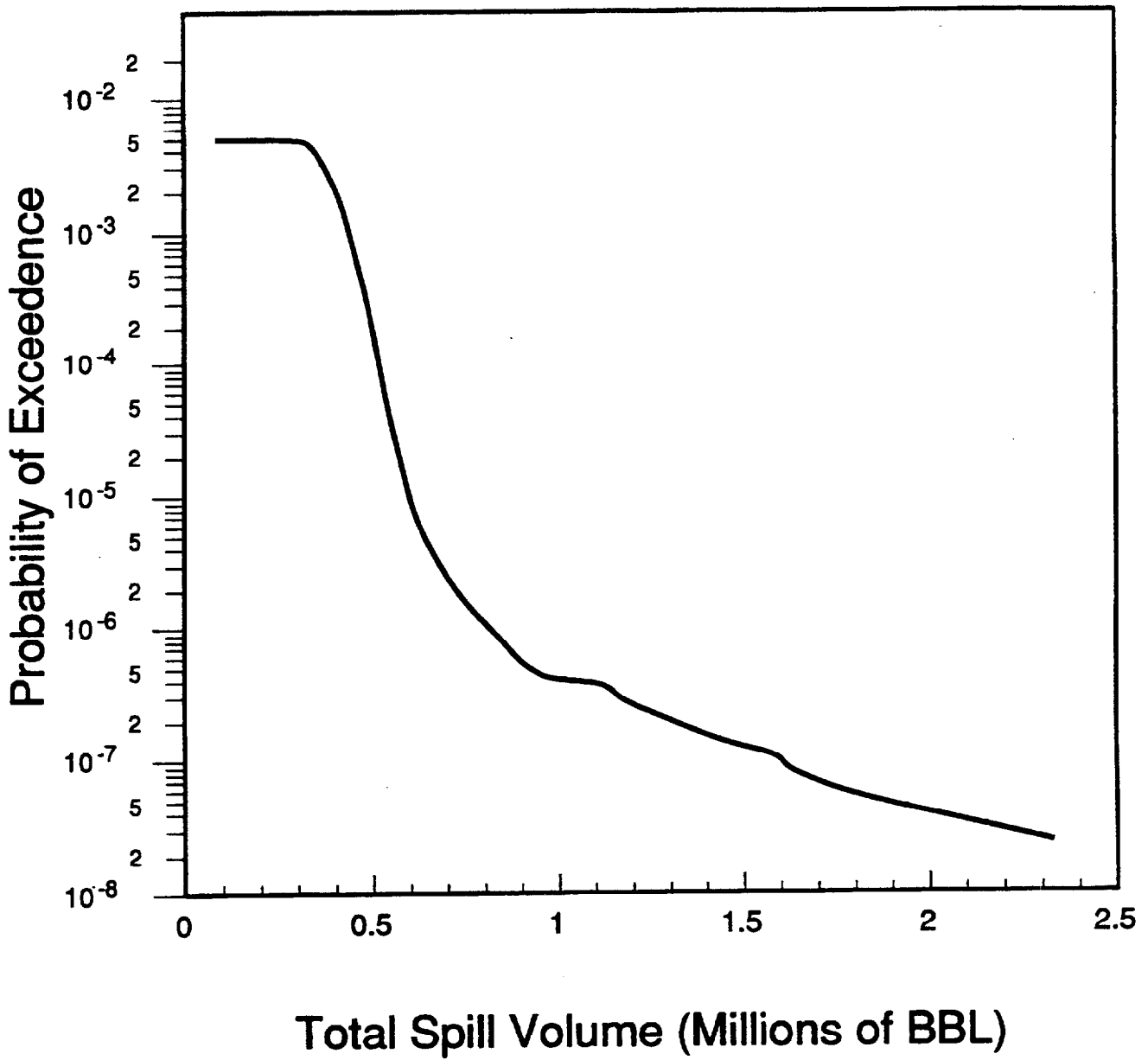


Figure 26: Risk of Oil Spills from a Large NMSZ Event

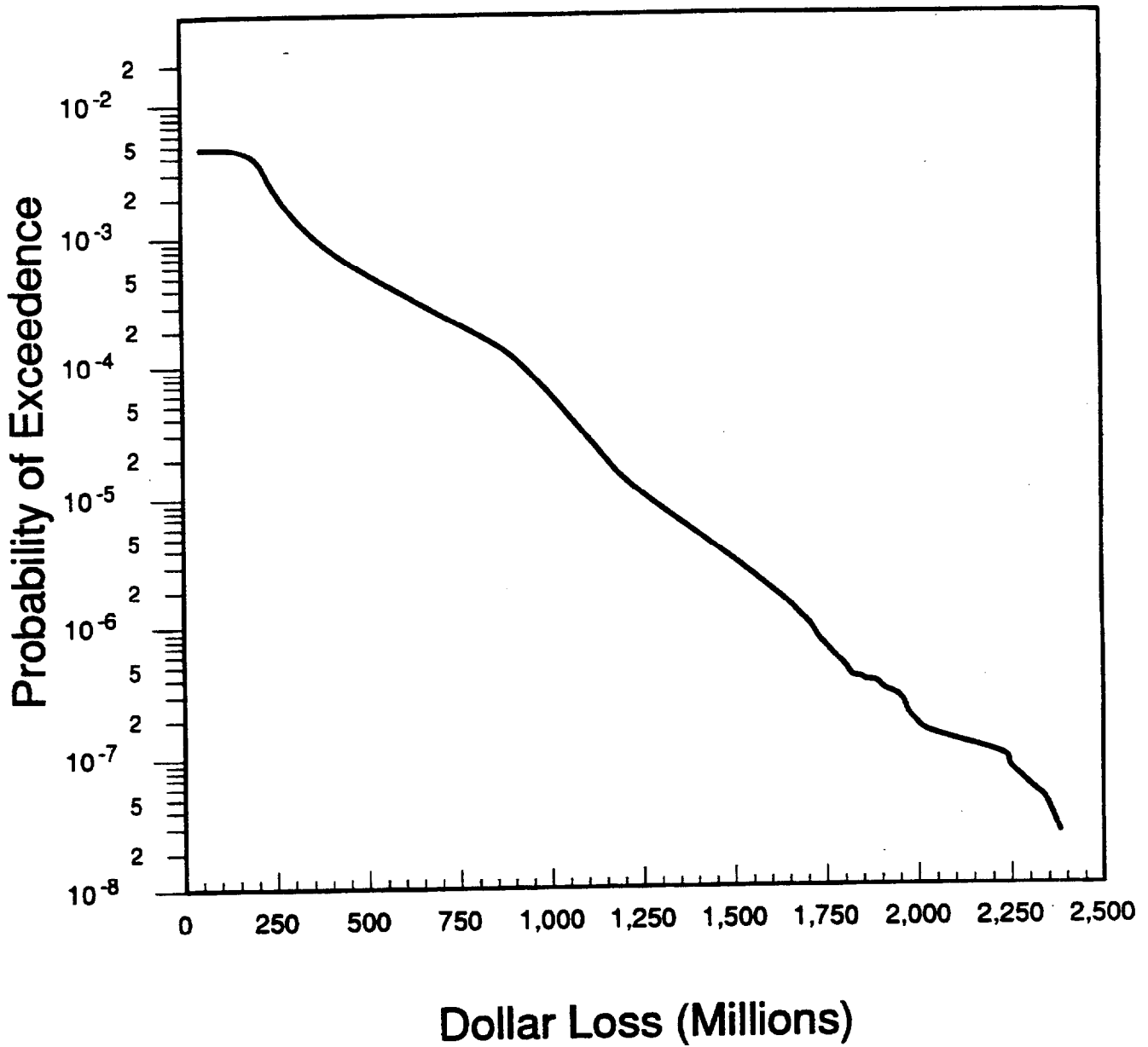


Figure 27 : Risk of Dollar Loss from a Large NMSZ Event